MICROCOPY RESOLUTION TEST CHART

NATIONAL BUREAU OF STANDARDS 1963

AD-A186 731

R87-926489-9

EXCIMER PLASMA DISPLAYS

DTIC
S ELECTE D
OCT 2 8 1987
D

FINAL REPORT

F. A. Otter, Jr. and W. L. Nighan

September 14, 1987

**UNITED
TECHNOLOGIES
RESEARCH
CENTER**

East Hartford, Connecticut 06108

R87-926489-9

EXCIMER PLASMA DISPLAYS

FINAL REPORT

F. A. Otter, Jr. and W. L. Nighan

September 14, 1987

**UNITED
TECHNOLOGIES
RESEARCH
CENTER**

East Hartford, Connecticut 06108

REPORT DOCUMENTATION PAGE		READ INSTRUCTIONS BEFORE COMPLETING FORM
1. REPORT NUMBER ARO 19508.2-PH	2. GOVT ACCESSION NO. ADA 186731	3. RECIPIENT'S CATALOG NUMBER N/A
4. TITLE *(and Subtitle)* Excimer Plasma Displays		5. TYPE OF REPORT & PERIOD COVERED Final Report Apr. 15, 1983–Sept. 14, 1987
		6. PERFORMING ORG. REPORT NUMBER R87-926489-9
7. AUTHOR(s) F. A. Otter, Jr. and W. L. Nighan		8. CONTRACT OR GRANT NUMBER(s) DAAG29-83-C-0013
9. PERFORMING ORGANIZATION NAME AND ADDRESS United Technologies Research Center Silver Lane East Hartford, CT 06108		10. PROGRAM ELEMENT, PROJECT, TASK AREA & WORK UNIT NUMBERS
11. CONTROLLING OFFICE NAME AND ADDRESS U. S. Army Research Office Post Office Box 12211 Research Triangle Park, NC 27709		12. REPORT DATE September 14, 1987
		13. NUMBER OF PAGES 60
14. MONITORING AGENCY NAME & ADDRESS(*if different from Controlling Office*)		15. SECURITY CLASS. *(of this report)* Unclassified
		15a. DECLASSIFICATION/DOWNGRADING SCHEDULE

16. DISTRIBUTION STATEMENT *(of this Report)*

Approved for public release; distribution unlimited.

17. DISTRIBUTION STATEMENT *(of the abstract entered in Block 20, if different from Report)*

NA

18. SUPPLEMENTARY NOTES

The view, opinions, and/or findings contained in this report are those of the author(s) and should not be construed as an official Department of the Army position, policy, or decision, unless so designated by other documentation.

19. KEY WORDS *(Continue on reverse side if necessary and identify by block number)*

Plasma displays; Plasma Panels; Flat Panel Displays; Excimer Fluorescence for Displays; Visible Excimer Fluorescence; XeO Fluorescence for Displays; XeF Fluorescence for Displays; $O(^1S)$ Quenching by $O_2(^1\Delta_g)$.

20. ABSTRACT *(Continue on reverse side if necessary and identify by block number)*

Under ARO Contract DAAG29-83-C-0013, United Technologies Research Center has conducted an investigation of the feasibility of utilizing visible excimer molecule fluorescence as a medium for flat panel plasma displays. Because large area ac plasma panels based on the Owens-Illinois Digivue™ design are the industry standard, panels of that type were used for test purposes throughout the program. The single most significant outcome of this research →

(Continued)

was the demonstration that visible fluorescence from XeO and XeF excimers can
be generated at a luminance level equivalent to that of the standard Ne-Penning
mixture, albeit at a lower luminance efficiency. It was found that a variety
of colors, varying continuously from pink through "white" to blue, can be
produced by combining neon line emission with broadband XeF emission in a mixture
comprised of Ne, Xe, F_2^{7} and Kr. A specific color or white is obtained by
changing the relative proportions of the rare gas mixture constituents. The
ability of XeF-based mixtures to produce emission over a large portion of the
visible spectrum suggests that color ac plasma panels may be possible through
use of an optical switching device or using an array of micro-filters to form
a pixel. Keywords —> '. field 19

ABSTRACT

Under ARO Contract DAAG29-83-C-0013, United Technologies Research Center has conducted an investigation of the feasibility of utilizing visible excimer molecule fluorescence as a medium for flat panel plasma displays. Because large area ac plasma panels based on the Owens-Illinois Digivue™ design are the industry standard, panels of that type were used for test purposes throughout the program.

A screening of potential excimer candidates indicated that XeO and XeF offered particular promise, and attention was focused on those two. The XeO and XeF excimers emit broadband radiation centered at 540 nm and 480 nm, respectively. The single most significant outcome of this research was the demonstration that visible fluorescence from these excimers can be generated at a luminance level equivalent to that of the standard Ne-Penning mixture, albeit at a lower luminance efficiency.

Our results with XeF are particularly significant. It was found that a variety of colors, varying continuously from pink through "white" to blue, can be produced by combining neon line emission with the broadband XeF emission in a mixture comprised of Ne, Xe, F_2 and Kr. A specific color or white is obtained by changing the relative proportions of the rare gas mixture constituents. The ability of XeF-based mixtures to produce emission over a large portion of the visible spectrum suggests that color ac plasma panels may be possible through use of an optical switching device or using an array of micro-filters to form a pixel. However, the key issue that will determine the viability of XeF displays is one of device lifetime using mixtures containing F_2. We conclude that in order to justify the additional effort and expense required to capitalize on XeF properties, a specific concept must emerge that has recognized potential for a full color or multi-color display.

i

E X C I M E R   P L A S M A   D I S P L A Y S

TABLE OF CONTENTS

I. INTRODUCTION

A. Background

Because of the uniquely favorable electrical and optical properties of glow discharges in neon, practically all commercially available flat panel plasma displays use a neon gas fill (Ref. 1). Indeed, in **ac plasma panels** the combination of the well known Ne-Penning mixture with the efficient, durable MgO electron emitting layer results in a very low firing voltage ($\sim$ 100 V) and a relatively high luminous efficiency ($\sim$ 0.5%) (Refs. 2 and 3). However, the neon transitions in the 580-700 nm region of the spectrum produce a reddish-orange color that is unsuitable for certain applications. Therefore, it would be highly desirable if gas mixtures capable of producing other colors could be found, while retaining the advantages of the now well developed ac plasma panel technology.

Since practically all gas discharges emit visible radiation, in principle, the easiest way to generate colors other than Ne orange is to change the gas mixture (Ref. 1). Ahearn and Sahni (Ref. 4) investigated helium-based Penning mixtures containing a variety of heavy rare gas and/or atmospheric dopants. When excited using a conventional ac plasma panel (MgO surface), those mixtures exhibited electrical characteristics and luminance levels generally similar to Ne-Penning mixtures, and violet, blue and white colors were obtained. However, in order to produce luminance levels comparable to that of a Ne-Penning mixture, excitation frequencies an order of magnitude higher were required. Thus, the luminous efficiency of such He-based mixtures is very low, a reflection of the fundamental fact that only a very small percentage of the fluorescence lies in the visible region.

Sahni (Ref. 5) also experimented with mercury seeded argon mixtures. Blue and green Hg line emission were produced at luminance and efficiency levels significantly higher than those of Ne-Penning mixtures operating at the same repetition frequency. Additionally, the firing voltage and memory margin were similar to those of conventional Ne-based mixtures. However, although the luminance and luminous efficiency levels were the highest ever observed for an ac plasma panel mixture, elevation of the panel temperature was required to optimize the Hg vapor concentration. Because of the strong dependence of Hg vapor pressure on temperature, both electrical and optical properties of the Ar/Hg panel exhibit variations in response to changes in temperature.

Additionally, other colors, and possibly multi-color emission, can be produced by using gas discharge generated electrons or UV radiation to excite phosphors (Ref. 1). This approach has been the subject of investigation for many years, and is currently being explored by several organizations. Although promising, phosphor excitation by low energy electrons/photons

requires a significantly more complicated plasma panel configuration than is characteristic of the Ne-filled panel. For that reason, in the present work we have concentrated on **alternate gas fills** intended for use in plasma panels of **conventional design**.

B. Excimer Mixtures

Over five years ago we began exploring the feasibility of utilizing **excimer** molecule fluorescence for ac plasma panel applications (Refs. 6 and 7). Excimers are excited species that are not stable in the ground electronic state; and therefore they are not present in the initial gas mixture. Presented in Fig. 1 is an illustration of a typical potential energy diagram for an excimer molecule. Because excimer molecules can be produced efficiently in electrically excited gases and have no stable ground state, for nearly twenty years they have been the subject of intense investigation for application as UV/visible laser media (Ref. 8). Indeed, low power UV excimer lasers are commercially available from several manufacturers, and the DoD currently supports many research and development programs directed toward scaling of excimer lasers to larger sizes and higher output energy levels. United Technologies Research Center has an extensive background in this area.

Our initial screening of excimer candidates having promise for display applications focused on molecules of the rare gas-halide and rare gas oxide classes. Excimers such as XeF, Kr_2F, Xe_2Cl and XeO exhibit strong emission in the visible region of the spectrum. Typical emission spectra for XeF, Xe_2Cl and XeO are presented in Fig. 2. The exceptionally broadband emission of these molecules reflects the strongly repulsive nature of the terminal state (Fig. 1). This is in contrast to the red and yellow line emission from the atomic transitions in Ne (Ref. 3), which result in the characteristic orange color of conventional plasma panels. However, a more significant difference between visible emission produced from a rare gas atom, e.g., Ne, and an excimer molecule is that the radiating excimer is not present in the initial, unexcited gas mixture. Rather, the excimer molecule must be produced by discharge generation of excited and ionized species which subsequently react to form the excimer.

Initial efforts to demonstrate "proof-of-principle" for the UTRC excimer display concept focused on the Xe_2Cl molecule producing blue-green emission centered at a wavelength of 490 nm (Ref. 6). That early work was encouraging, resulting in a U.S. patent (No. 4,549,109), and provided the basis for the present contract which was directed toward investigating the **practical feasibility** of utilizing excimer molecule fluorescence for plasma panels of conventional design. Under the present contract, our research has been focused on two excimer molecules, XeO and XeF, both of which exhibit characteristics of special importance for displays. The green XeO emission is

Energy

A + B*

AB*

hν

A + B

Internuclear separation
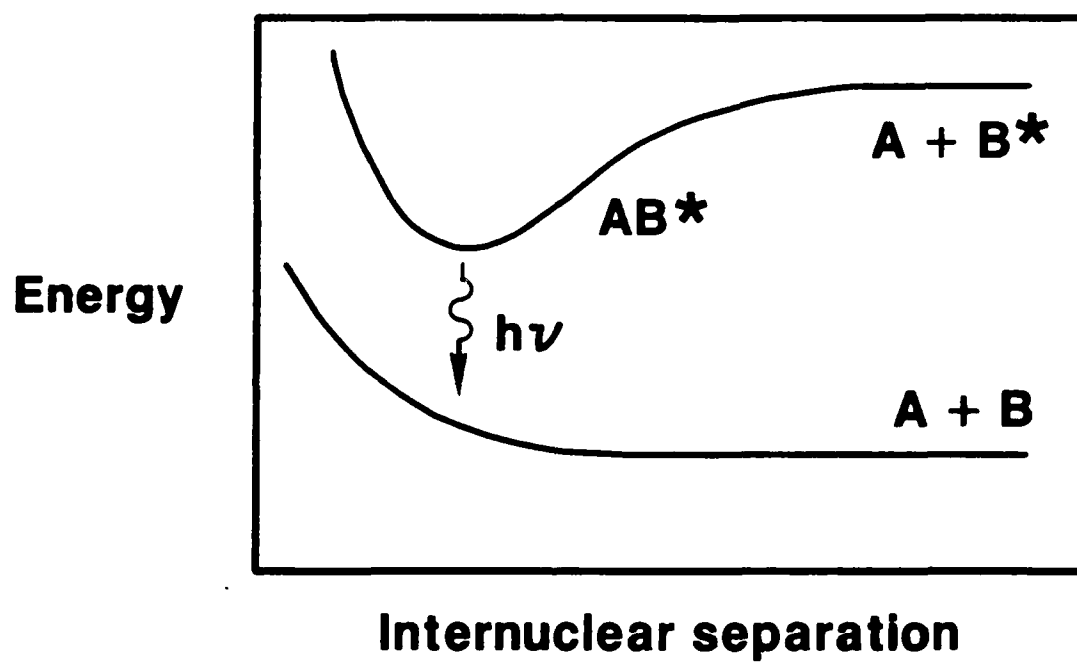
Figure 1. Typical excimer molecule potential energy diagram.
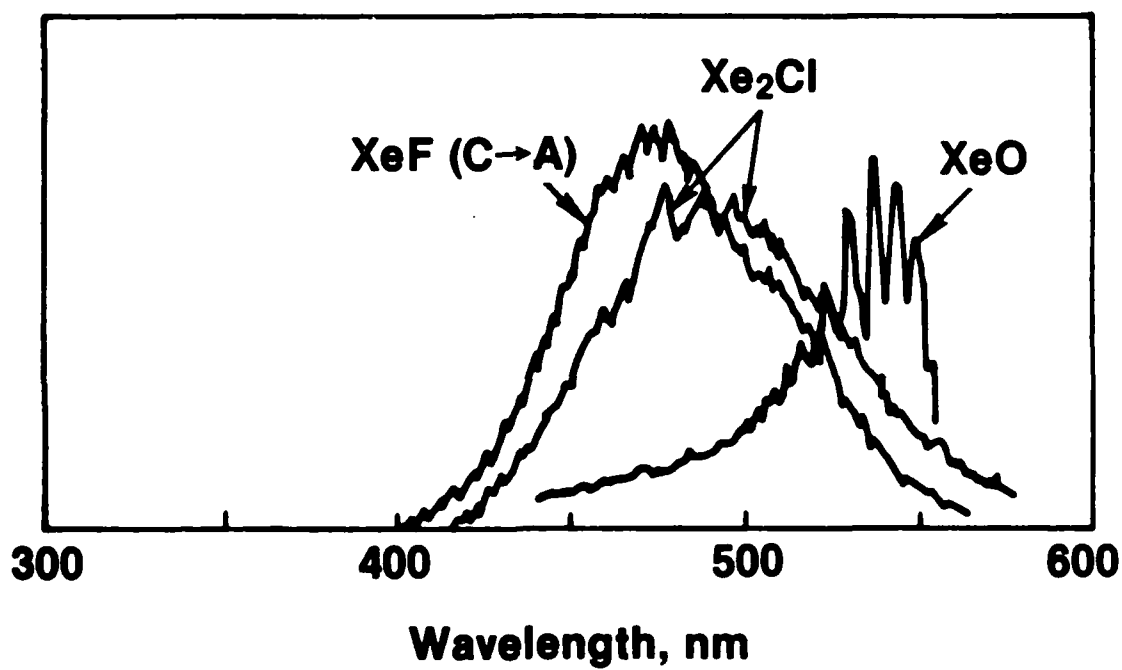
Figure 2. Representative emission spectra for XeF, Xe_2Cl and XeO excimer transitions.

4

centered at 540 nm (Fig. 2) and provides an exceptional match to the response of the eye. The C→A transition of XeF is in the blue-green region centered at 480 nm. The XeF excimer can be produced with high efficiency in an electric discharge, therefore offering promise for high brightness and efficiency.

Section II of this report presents a discussion of the experimental apparatus and procedures typical of our work with both XeO and XeF. Specific details and results for XeO and XeF are presented in Sections III and IV, respectively. The current state of affairs along with discussion of our conclusions is presented in Section V with a prognosis for future development.

II. EXPERIMENTAL APPARATUS

A. AC Plasma Panel

All experiments were performed using standard production ac plasma panels that are basically identical in design to those manufactured by United Technologies' Norden Systems for several Army C^3 programs. Minor modifications (described in Sec. IV) were made to perform experiments using excimer mixtures. Figure 3 shows a photograph of a panel manufactured for UTRC by Electro Plasma, Inc., (EPI), one of Norden's second source suppliers of panels that use a Penning mixture. The overall dimensions of the panel are 33 cm x 20 cm with an internal active display area of 25 cm x 12.5 cm. External leads for electrically addressing the pixels are visible around the edges. Also visible is a sealed glass tubulation used in the original manufacturing process to bake and evacuate the gas space inside the panel and to admit the desired pressure of gas – a Penning mixture comprised of Ne + 0.15% Xe (or Ar) at a total pressure of 375 torr. Panels were mounted on a "homemade" stand as shown in order to facilitate electrical and optical measurements.

Figure 4 is a schematic illustration of the construction of an ac plasma panel of the Owens-Illinois Digivue™ design. Two heavy glass plates 6 mm thick are sealed around the edges to form a gas space for the plasma-sustaining gas mixture. Small glass spacers (about 50 mm apart) are used to keep the interior spacing constant at about 100 microns. Parallel metal electrodes run horizontally on one glass plate and vertically on the other with the cross-over regions defining individual pixels. The electrodes are about 75 microns wide and are spaced on centers about 0.5 mm apart. Half of the electrodes are addressable from the left and right (top and bottom) sides of the panel, resulting in about 400 pixels per cm^2. On the right side of Fig. 4 is shown the details of the inner-surface layer of each glass plate. On a standard panel there is a thin (typically 5 microns) dielectric (quartz) deposited over the glass substrate (and electrodes), over which is deposited an additional protective layer of MgO ($\sim$ 0.2 microns) which serves as a good electron emitter for Penning mixtures. The MgF_2 layer indicated in Fig. 4 is a thin passivation layer formed when F_2 has been admitted to the panel for XeF experiments to be described in detail in Section IV. Details of the ac operation of such a panel are discussed thoroughly elsewhere (Ref. 1), and we will draw heavily on that work, when necessary, in order to discuss operating parameters such as on/off voltages, voltage "margins" (i.e. Von-Voff), sustain voltages, and voltage repetition rate (operating frequency).

Figure 5 is a schematic of pixels on an enlarged scale. The "light collection circle" shown was chosen (by adjusting the optics in our single pixel luminance measuring apparatus) to be 0.006" (152 microns) in order to approximate the resolution of the human eye at a viewing distance of 21 inches (i.e., 1 minute of arc).
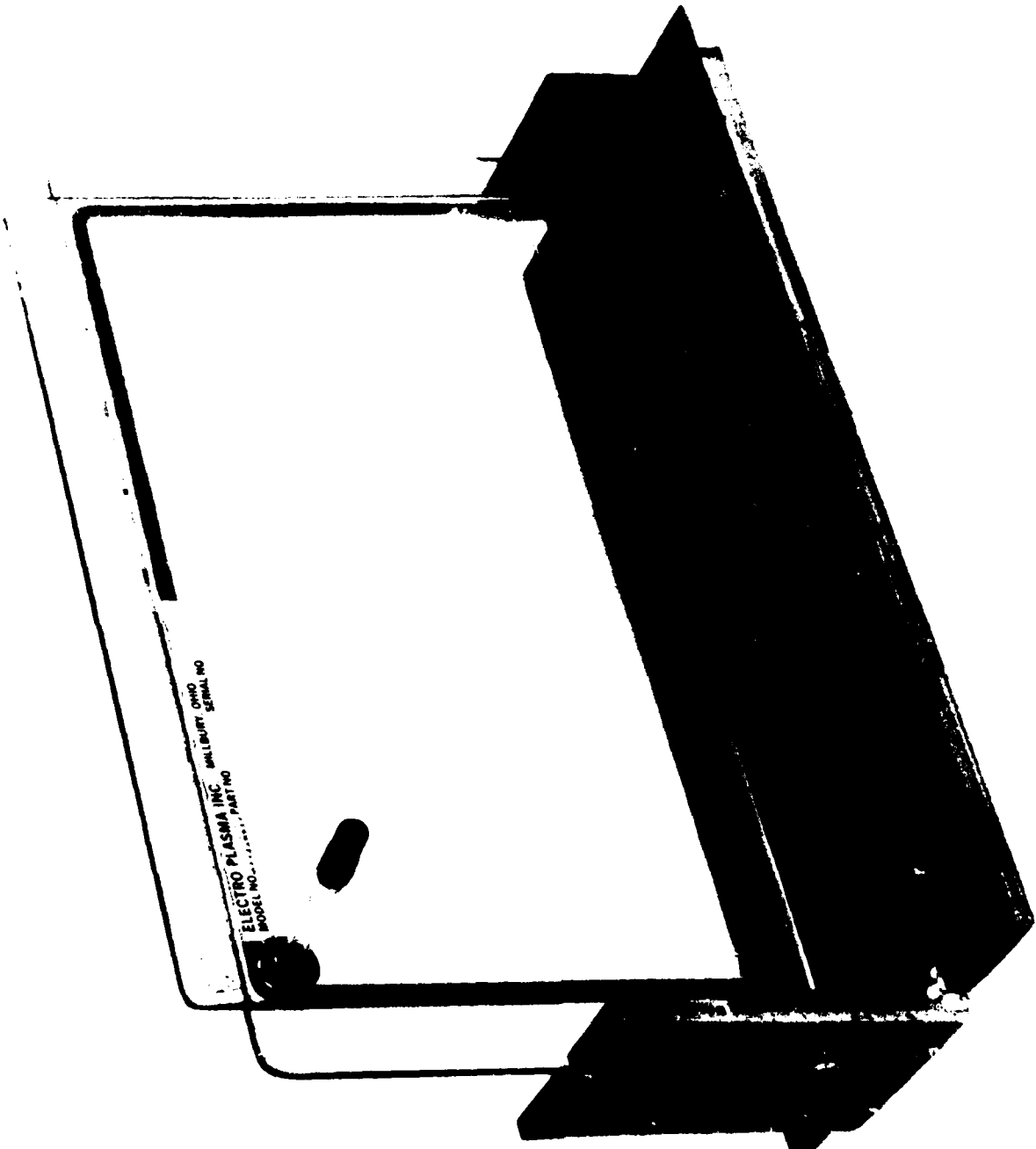
Figure 3. Plasma panel of the type manufactured by Electro-Plasma, Inc. and United Technologies' Norden Systems for use in several Army C^3 systems currently in production. Such panels are of the Owens-Illinois Digivue™ design (Ref. 1).

87 - 87E

87 - 8 - 68 - 1

7
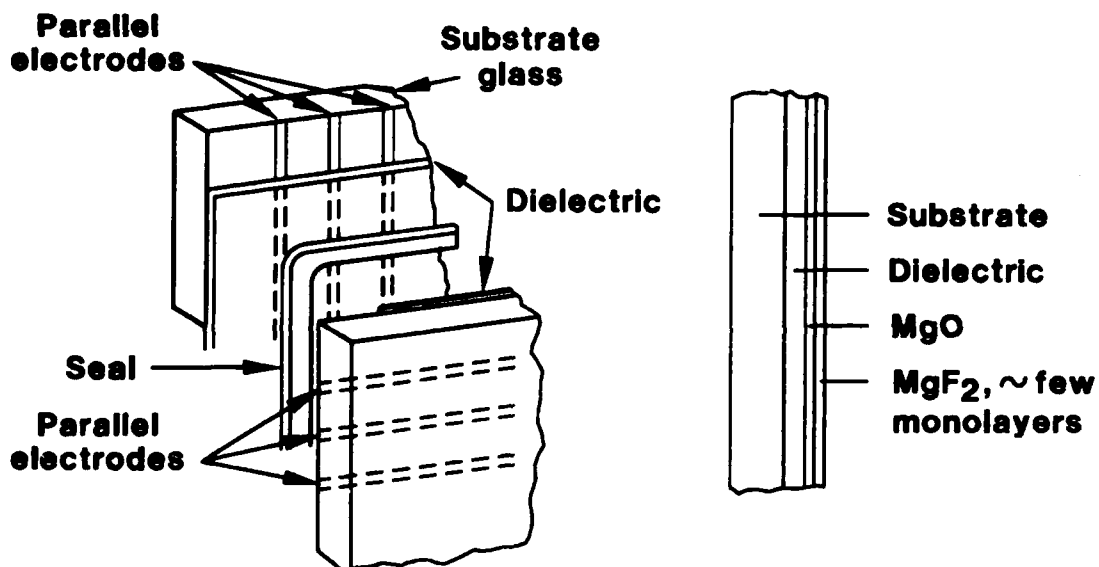
Figure 4. Schematic illustration of a plasma panel in an exploded view. The MgF_2 covering the MgO layer as illustrated to the right is a passivation layer of a few monolayers thickness. The MgF_2 layer results from passivation and operation with mixtures containing F_2 as described in Section IV-B.
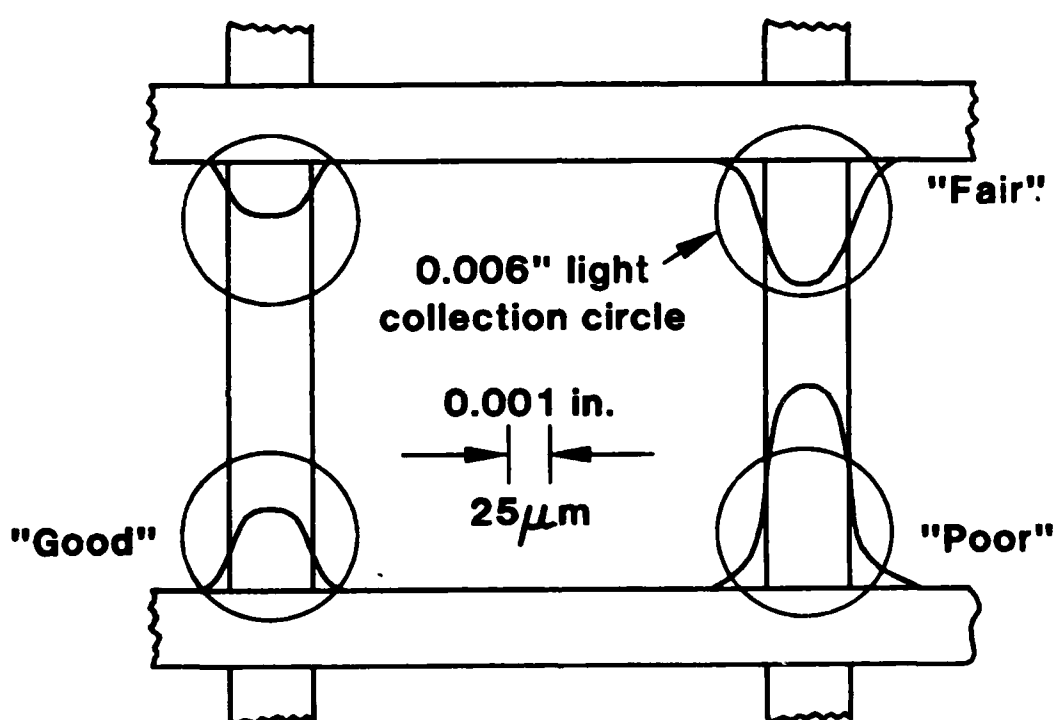
Figure 5. Illustration of plasma panel pixels showing the location of the collection circle for luminance measurements, and also indicating the plasma "shapes" relative to the collection circle as described in Section IV-C.

B. Gas Handling

Figure 6 shows the gas handling system. The system was constructed largely of ultra-high vacuum components in order to maintain maximum cleanliness and gas purity when preparing test mixtures. The main chamber was pumped with a CIT-Alcatel turbopump system that could routinely produce pressure in the 10^{-7} to high 10^{-8} torr range. Pressures were monitored with a Varian Model 843 gage controller and a Varian Model 928-1000 Residual Gas Analyzer (RGA). Higher pressures (when preparing mixtures) were measured with Wallace-Tiernan dial gages (0-50 and 0-1000 Torr) which could be isolated with valves as required. A liquid nitrogen (LN_2)-trapped forepump was used in parallel with the turbopump for initial high flow pump-downs from near-atmosphere pressures. Various high purity gases for preparing mixtures could be introduced through four valved inlet ports to the main mixing chamber.

The main mixing chamber had a rotating vane-magnet assembly in the chamber which was driven by means of an external rotating magnet (in a hotplate). The moving vanes served as a "fan" to facilitate mixing of multiple component mixtures in the chamber. A fifth port/valve assembly served to introduce gases into the plasma panel, which also had a parallel pumping path available to the turbopump. Connection of the gas line to the panel was made through the pump-out port shown in Fig. 3. The actual assembly was accomplished in a glove box to prevent air or water vapor from entering the panel gas space. A typical operating procedure was to pump out the mixing chamber, gages, and panel to a pressure of 10^{-7} Torr or less prior to each experiment. Gases were then introduced into the mixing chamber in the desired proportions and mixed for a suitable length of time. We found that 1/2 hour of mixing was adequate, but generally the gases were mixed for an hour or more. After mixing, gas was admitted to the evacuated panel for experimentation. Generally a gas charge was admitted to the panel, and then the panel was again pumped hard before putting in the final gas charge -i.e., the panel was "flushed" with each mixture before taking data.

Figure 7 shows the overall experimental arrangement with a panel in place. Shown in the background is a dc power supply and a pair of UTRC-constructed square-wave generators for applying the square wave ac voltage across the panel. A Tektronix oscilloscope was used to track the waveform and monitor other electrical signals as described below. The square-wave generator system can produce square waves of amplitude up to 450 volts (900 V, P-P) at frequencies from about 6 kHz to 500 kHz. A pair of IRCO Model 956SUT High Voltage Pulse Generators were used for experiments on the effects of waveform on performance.
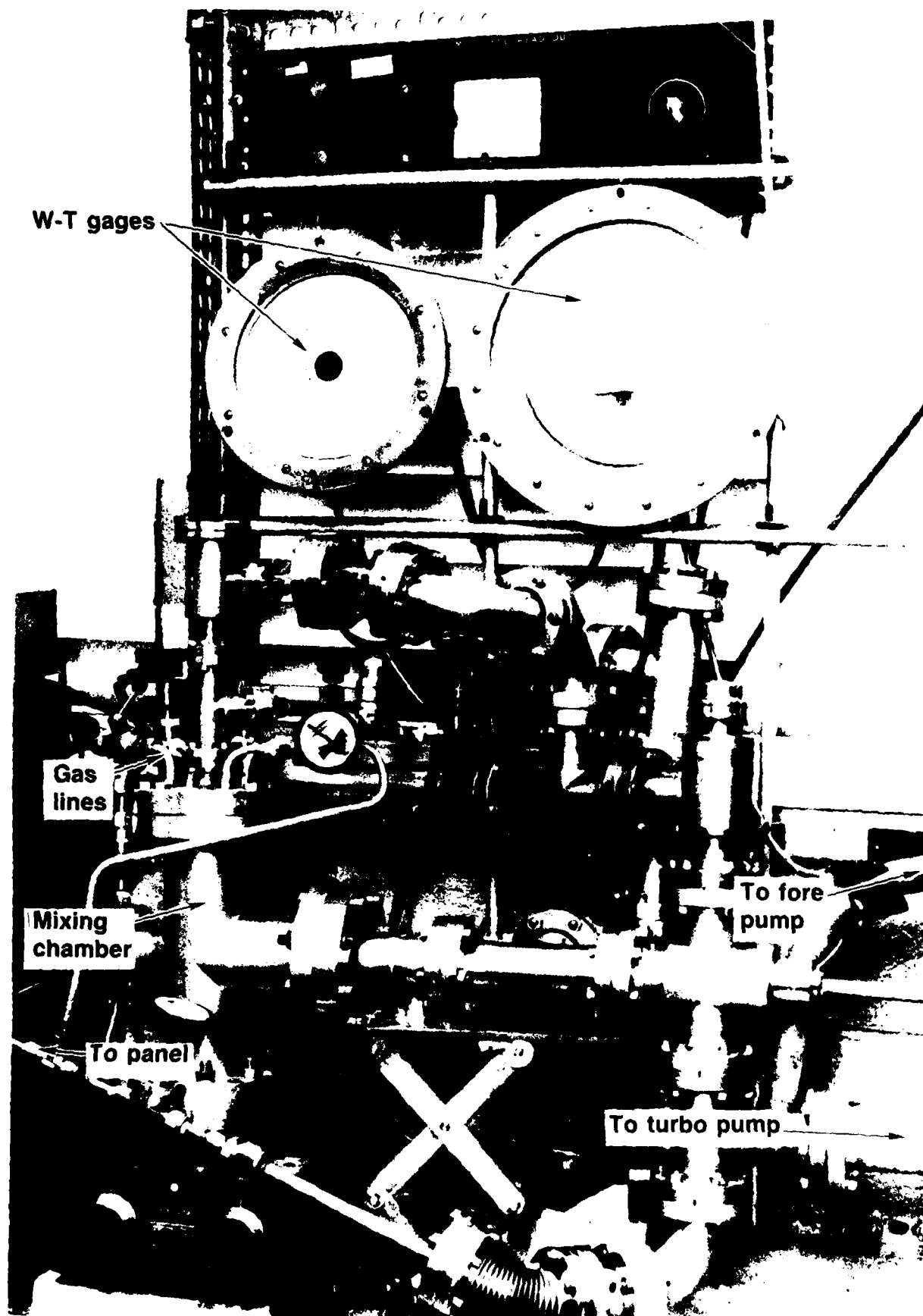
Figure 6. Close-up view of gas handling system.
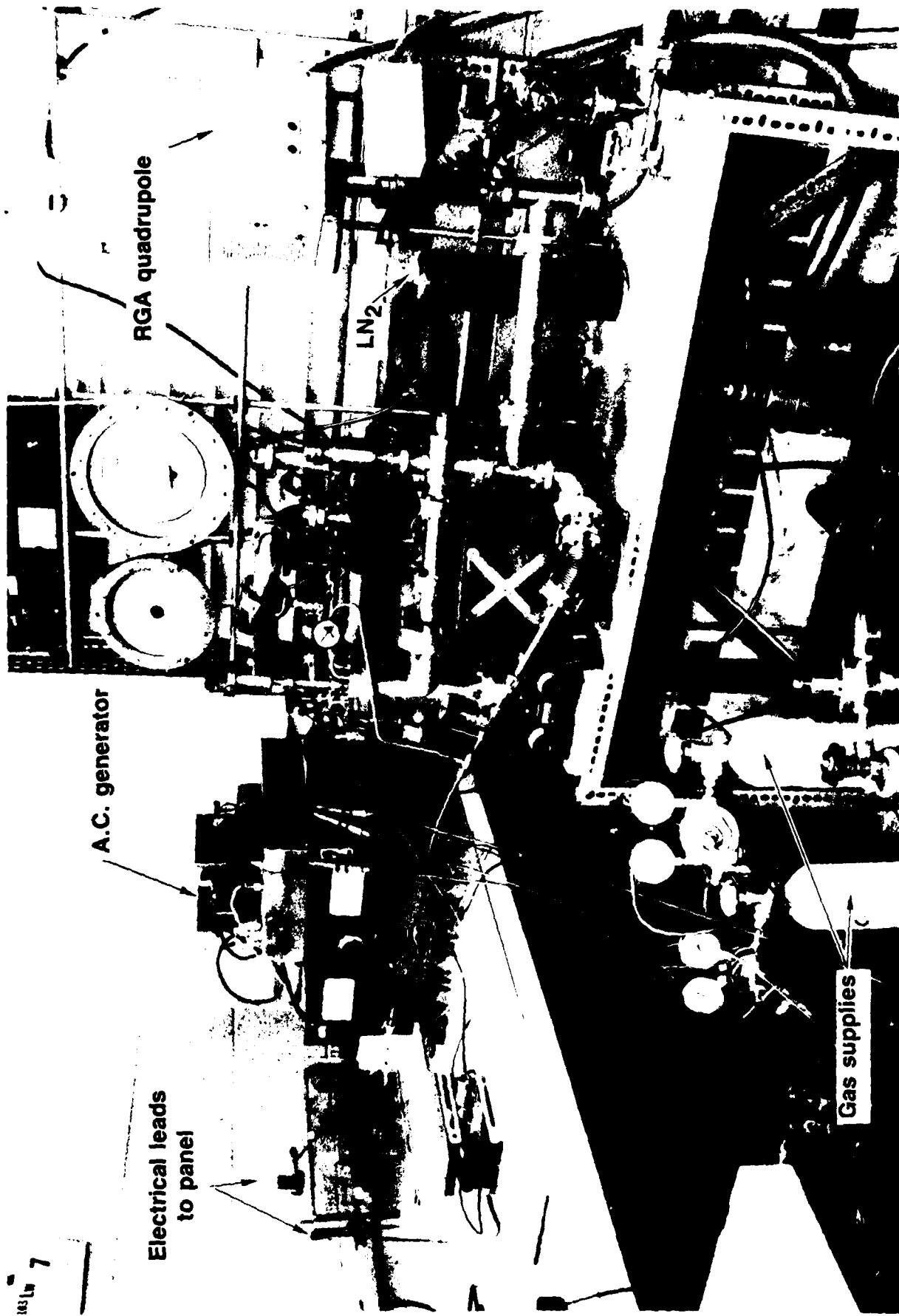
Figure 7. Overall experimental arrangement with a test plasma panel attached to the gas handling system.

RGA quadrupole

LN$_2$

A.C. generator

Electrical leads to panel

Gas supplies

87-87A-3

87 8 68-3

12

C. Optical Measurements

Individual pixel luminance measurements were made using a UDT Model 255 Si detector connected to a UDT Model 550 Optical Power Meter. On the detector was mounted a UDT Model 1157 Photometric Filter. A UDT 1120 Reflex Viewing telescope was adjusted to focus on a 152 micron (0.006") diameter circle as illustrated in Fig. 5. Power meter readings in dB were converted to relative luminance and eventually related to units of foot lamberts using a standard Norden Systems' panel as a reference. Sometimes, for convenience, the detector-filter assembly was simply placed against the lighted patch on a panel (typically a patch of 1024 lighted pixels about 3 cm square), and readings taken in dB. Careful calibration tests showed that those measurements tracked the individual pixel measurements well.

During the latter stages of the program a Minolta Chromameter II was acquired for measurement of specific colors. This instrument yields relative luminance and color coordinates (1931 CIE or 1976 CIE standards) in a single measurement. Luminance values so obtained were in accord with those obtained using the UDT instrument, so that eventually the Chromameter was used exclusively.

For spectroscopic measurements, a Jarrell-Ash 82-020 0.5 meter McPherson type scanning monochromater was used, which was coupled to a lighted test patch by means of a sapphire light pipe. The detector was a UDT-555 "Photop" silicon photodiode with a built-in op-amp, the output of which was recorded on a Mosley 680 chart recorder. Scan rates were typically 250 Å/min. The "Photop" was also used for measuring the time evolution of light pulses as discussed in Secs. III.

III. XeO EXCIMER RESEARCH

The XeO excimer is produced in electrically excited mixtures comprised of Xe and O_2. Both Xe and O_2 are species that have been used in plasma panels (Refs. 1 and 4), and should be compatible with interior panel materials. For that reason our attention was focused first on XeO excimer emission.

A. XeO Kinetics

The long-lived (~1 sec) $O(^1S)$ atom, produced by dissociative excitation of O_2 or by excitation of ground state oxygen atoms, is known to form transient radiating molecular species with the rare gases (Refs. 9, 10), i.e.,

$$O(^1S) + 2RG \rightarrow RGO^* + RG \tag{1}$$

The transition probability of the rare gas-oxide excimer so formed is five-to-six orders of magnitude larger than that of the oxygen $^1S \rightarrow ^1D$ green auroral transition at 557.7 nm (Refs. 9, 11). Thus, in certain rare gas-oxygen mixtures, this collisional-radiative process results in a broadened and slightly shifted $O(^1S)$ emission, which is greatly enhanced in intensity and which occurs in the visible region. Vibrational analysis of rare gas oxide emission spectra shows that the ArO and KrO excimers have a very small binding energy ($\ll$ kT), while XeO is bound by ~0.06 eV. Because of its relatively large binding energy, over the years XeO has been the subject of investigation for use in laser applications (Ref. 12). For the same reason, in the present work XeO was considered a prime candidate as a display medium.

The schematic potential energy curves for the XeO states (Ref. 11) of importance are shown in Fig. 8, which illustrates the $^1\Sigma^+ - ^1\Sigma^+$ green band transition and also shows the very weak ($<$ 0.1 eV) bonding of the radiating $2^1\Sigma^+$ XeO state. Presented in Fig. 9 is the XeO $2^1\Sigma^+ - 1^1\Sigma^+$ "green-band" emission spectrum. Also shown for comparison are the scotopic (dark adapted) and photopic eye response curves, along with the emission spectrum of P-1 (or GJ) phosphor (Ref. 1). Clearly, the XeO emission spectrum is exceptionally well matched to the response of the eye under all ambient viewing conditions.

1. XeO Formation

The $XeO(2^1\Sigma^+)$ excimer (Fig. 8) is produced by electrical excitation of relatively high pressure ($\tilde{>}$ 1 atm) Xe containing a small (~0.1%) concentration of an oxygen bearing species, O_2 in the present case. Under such conditions
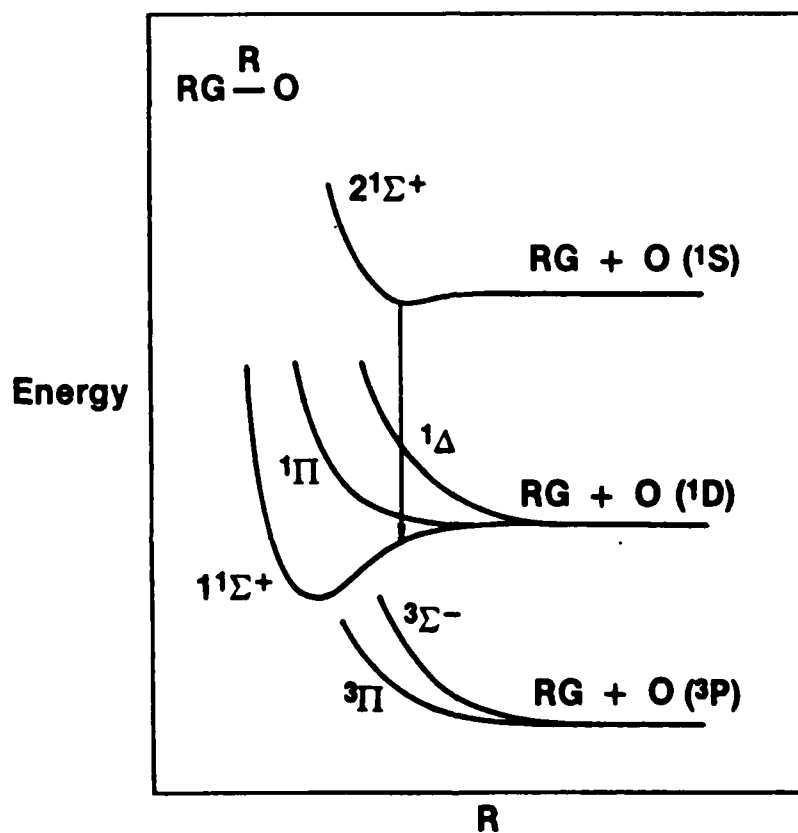
Figure 8. Potential energy curves for the rare gas-oxide states arising from RG + $O(^3P, ^1D, ^1S)$. The $^1\Sigma^+ - ^1\Sigma^+$ transition resulting in XeO green band emission is indicated by the arrow.
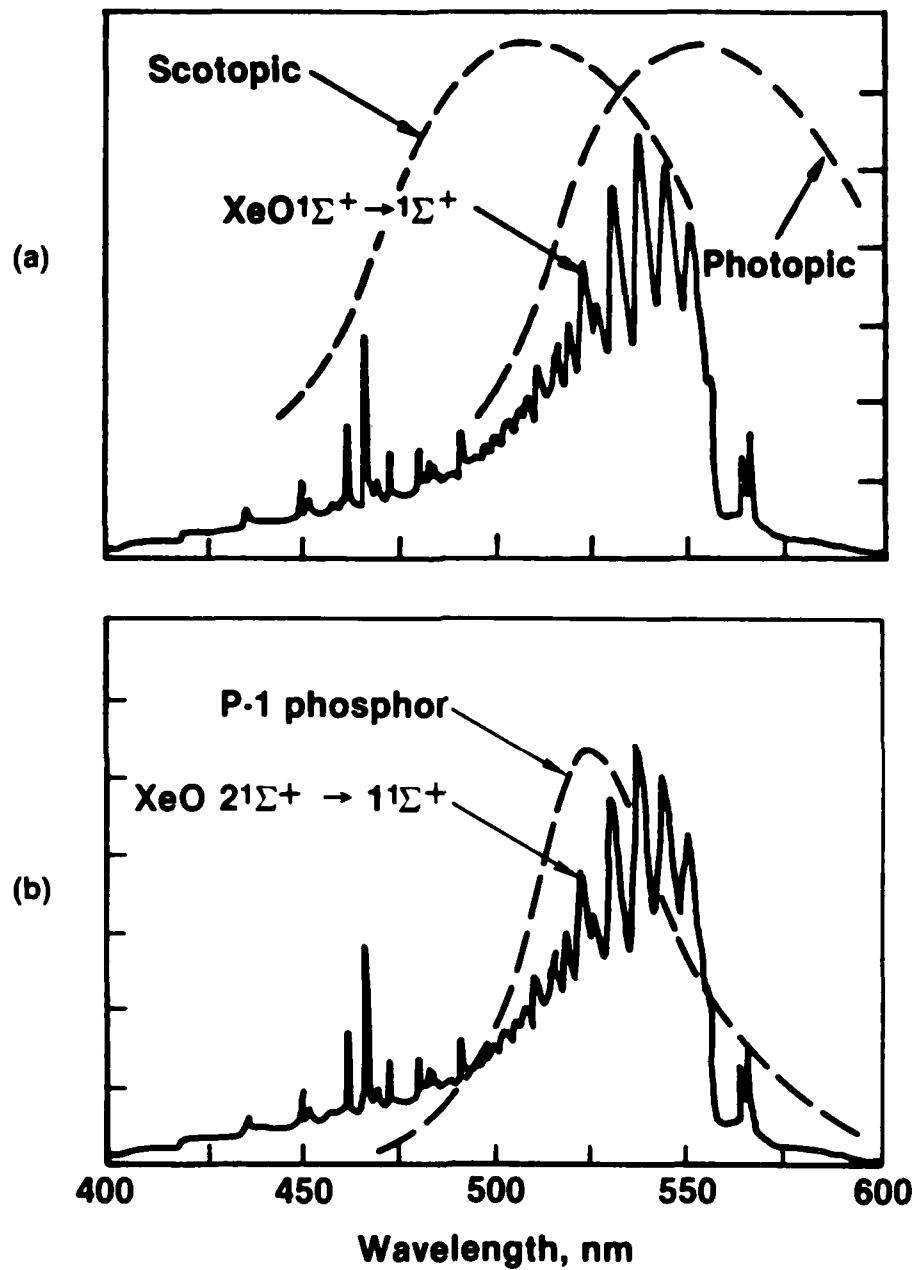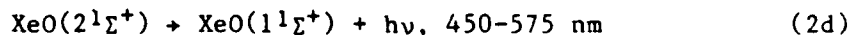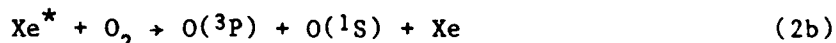
Figure 9. XeO green band emission spectrum. Also shown for comparison are the scotopic and photopic eye response curves (a), and the emission spectrum of P-1 phosphor (b).

discharge modeling shows that the **primary** reactions in the excitation sequence resulting in XeO green-band emission are as follows:

$$e + Xe \rightarrow Xe^* + e \qquad (2a)$$

$$Xe^* + O_2 \rightarrow O(^3P) + O(^1S) + Xe \qquad (2b)$$

$$O(^1S) + 2Xe \rightleftarrows XeO(2^1\Sigma^+) + Xe \qquad (2c)$$

$$XeO(2^1\Sigma^+) \rightarrow XeO(1^1\Sigma^+) + h\nu, \ 450\text{-}575 \ nm \qquad (2d)$$

For typical electric discharge conditions, Xe^* formation is a very efficient process. Moreover, for the conditions of interest here, the primary loss process for Xe^* is dissociative quenching by O_2. Unfortunately, the principal products of $Xe^* - O_2$ dissociative quenching are $O(^1D)$ and $O(^3P)$, rather than $O(^1S)$, the precursor of $XeO(2^1\Sigma^+)$ (Ref. 13). In fact, the branching fraction for $O(^1S)$ formation has been shown to be only ~1%, a factor significantly limiting the potential luminous efficiency of an XeO-based display. Other, more efficient, sources of $O(^1S)$, such as N_2O, have been used with considerable success in laser applications, with photodissociation of N_2O providing an efficient source of $O(^1S)$ (Ref. 12). However, for display applications, N_2O photodissociation does not appear to be a practical means of producing $O(^1S)$, and irreversible reactions occur which would also render use of N_2O difficult.

2. O(^{1}S) Loss

For Xe pressures of the order of an atmosphere the equilibrium between $XeO(2^1\Sigma^+)$ and $O(^1S)$ is established on a ~10 nsec time scale. Moreover, because $XeO(2^1\Sigma^+)$ is bound by only ~0.06 eV, the equilibrium favors $O(^1S)$. For example, for XeO in one atmosphere of Xe at room temperature, XeO represents only ~2% of the total XeO $(2^1\Sigma^+) \rightleftarrows O(^1S)$ population. Nonetheless, because the radiative transition probability of XeO is more than 10^6 times greater than that of $O(^1S)$, the desired XeO green-band emission is by far the dominant **radiative** loss of the XeO $\rightleftarrows O(^1S)$ system. In order to utilize this characteristic efficiently it is essential that collisional deactivation of $O(^1S)$ by medium constituents be small compared to the loss of $O(^1S)$ though the XeO green-band transition.

Electric discharge excitation of O_2 gas mixtures containing O_2 is an efficient source of metastable $O_2(a^1\Delta_g)$ which has a lifetime of approximately sixty minutes. Since $a^1\Delta_g$ is exceptionally difficult to quench by either atomic or molecular species or surfaces, in discharge excited O_2 the $a^1\Delta_g$ population rapidly reaches an equilibrium level typically 5-20% of the ground state O_2 concentration (Refs. 14-17). Relatively recently it

has been learned that $O_2(a^1\Delta_g)$ is a strong deactivator of $O(^1S)$, having a rate coefficient of $\sim 2.0 \times 10^{-10}$ $s^{-1}cm^3$ (Refs. 17-19). For O_2 fractional concentrations of a few tenths of one percent in Xe at atmospheric pressure, this implies that the collisional deactivation rate of $O(^1S)$ by $a^1\Delta g$ will have a characteristic time of $< 10^{-6}$ sec, compared to the effective radiative lifetime of the $O(^1S) \rightleftarrows XeO$ combination of $\sim 10^{-5}$ sec under the same conditions. As regards luminous efficiency, this is very significant, since it means that on the order of 90% of the $O(^1S)$ produced will be lost by collisional processes rather than by way of XeO radiation.

Figure 10 provides confirmation that $O(^1S)$ collisional quenching is dominant for the conditions to be discussed in subsequent sections. That figure shows the measured temporal decay of XeO fluorescence and that computed assuming an quasi-equilibrium $O_2(a^1\Delta_g)/O_2$ ratio of 0.15, a value typical of discharge excited media (Refs. 14-17). The computed value is normalized to the data at the peak. Clearly, the computed temporal evolution of XeO fluorescence is in very good agreement with that observed experimentally, both indicating a characteristic decay time of ~ 400 nsec, in marked contrast to the effective ~ 10 µsec XeO-$O(^1S)$ radiative lifetime for these conditions.

B. Experimental Procedures

Mixtures comprised of Xe and O_2 were prepared at pressures of ≥ 600 Torr and mixed using the procedures described in Section IIB. For a desired panel operating pressure, P, the pressure in the mixing chamber was adjusted to a value $\sim 3.0\%$ above P, and then the valve was opened to admit the mixture to the previously evacuated panel. Early experimental results were not reproducible until we realized the importance of the interaction of the plasma and the MgO surface, which altered both the O_2 content of the gas phase and the stoichiometry of the MgO surface. Subsequent measurements were then made only after long prior conditioning of the panel surface.

Measurements were carried out using one of two surface preparation conditions to be referred to as "high" conditioning and "low" conditioning. "High" conditioning involved saturating the oxygen content of the MgO surface by operating the panel for about an hour with a Xe-O_2 mixture containing about 5% O_2, an O_2 level found sufficient to saturate the surface. "Low" conditioning involved a similar treatment with pure Xe which resulted in an MgO surface deficient in oxygen. It was also apparent that small amounts of contaminants could drastically alter results; in that regard, RGA measurements of gas composition following each run provided a useful measure on the quality of experimental results.
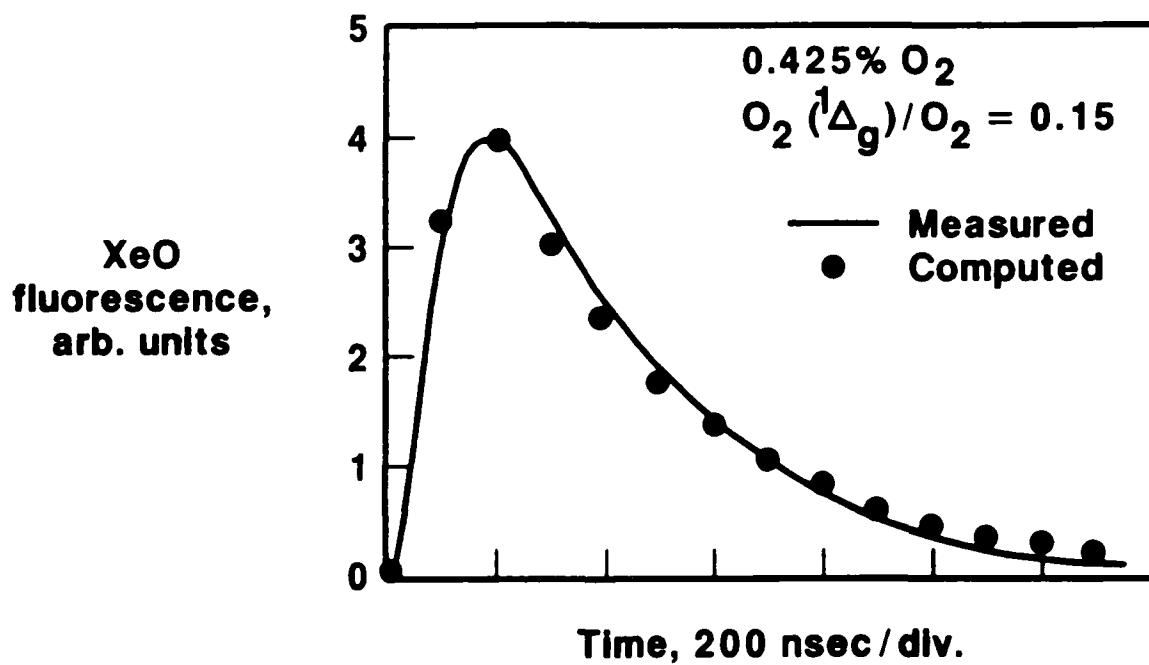
Figure 10. Measured and computed temporal decay of the XeO
green band fluorescence for a Xe-0.3% O_2 mixture at a
pressure of 500 Torr. The mixture was excited in a plasma
panel with the operating repetition frequency at 200 kHz.

C. Experimental Results

1. Paschen Curves

Figure 11 shows Paschen curves for a $Xe-O_2$ mixture initially containing about 0.2% O_2. Provided panel surface conditioning was complete, the curves for other O_2 concentrations were not very different. Figure 11 shows clearly that the voltages for "low" conditioning are lower than for "high", especially the "on" voltages (ignition). "On" voltages were not measured for pressures corresponding to voltages exceeding ~440 volts because of the limitation of our square wave generator. We were able to measure "off" voltages for higher pressures by first turning up the voltage and then admitting the gas slowly to get a "light" as the pressure in the panel passed through the minimum in each Paschen curve. Once ignited, the panel remained lit as the pressure increased to the preselected value. The observed "bump" in the "off" curve for pressures near 200 Torr for "low" conditioned panels was found to be reproducible, but is not understood. Another observation apparent from Fig. 11 is that the voltage margins (Von-Voff) and operating voltages are high, a factor resulting in a high power consumption.

2. Luminance Measurements

Measured luminance values were found to be dependent both on prior conditioning and on time of operation following the initial "light". Figure 12 shows a typical luminance time dependence. The initial decrease in luminance, an effect believed due to gas heating, was followed by an eventual saturation level. These time regimes are referred to as "early" and "late" in the figure and in subsequent discussion.

Figure 13 shows the luminance vs. initial oxygen concentration for a Xe pressure of 500 torr and a repetition frequency of 200 kHz for a "low conditioned" panel. Over the complete range of test concentrations, "late" operation, occurring ~10 min. after test initiation (Fig. 12), results in a luminance level about 1/2 as high as "early" operation. The peak luminance was found to occur at about 0.25% O_2 for both time regimes. Figure 14 shows luminance data for "late" operation for "high" and "low" conditioned panels. "High" conditioning moves the luminance vs. concentration peak down to an initial O_2 concentration of ~0.1%. Moreover, for the "high conditioned" case, the XeO luminance is essentially the same with no O_2 initially present in the mixture. This result clearly shows that the exchange of O_2 between the gas phase and the MgO surface is very significant, resulting in an O_2 gas phase concentration nearly the same as required to optimize XeO emmission.

The data of Fig. 14 were obtained using a different set of test pixels than those shown in Fig. 13. Comparison of these figures shows that the "low conditioned" results are somewhat different for the two cases. Thus, it
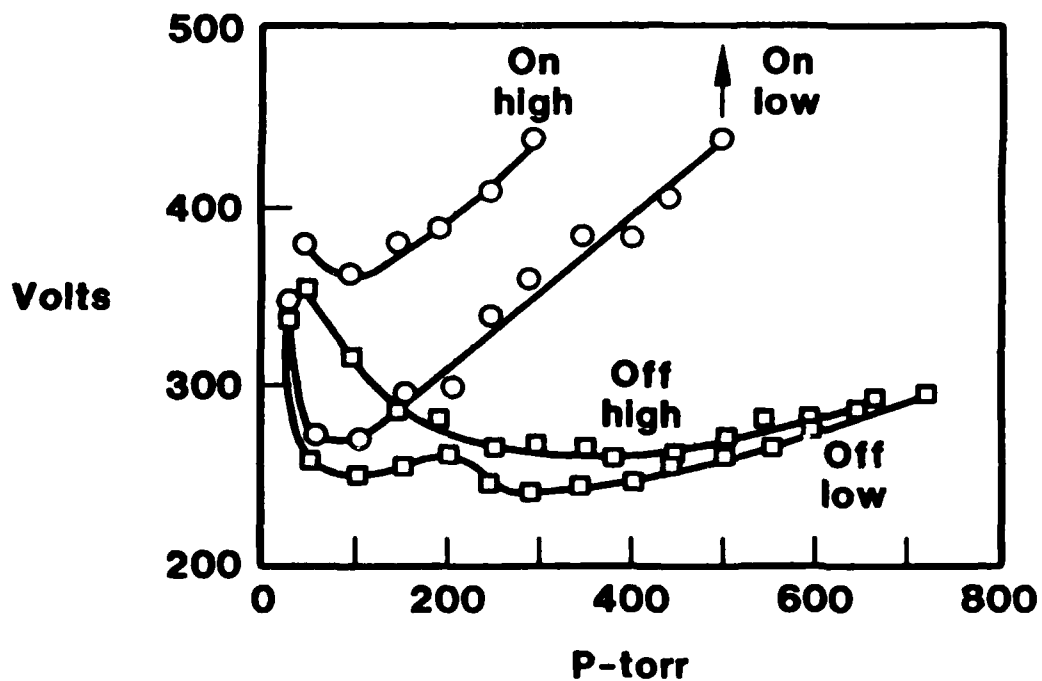
Figure 11. Paschen curves for a 500 Torr Xe-O_2 mixture having an _initial_ O_2 fill fraction of 0.2%. "On" and "off" refer to panel ignition and extinction, while the designations "high" and "low" refer to the panel preparation condition as described in Section III-B. "On" voltages higher than 440V could not be obtained because of power supply limitations.
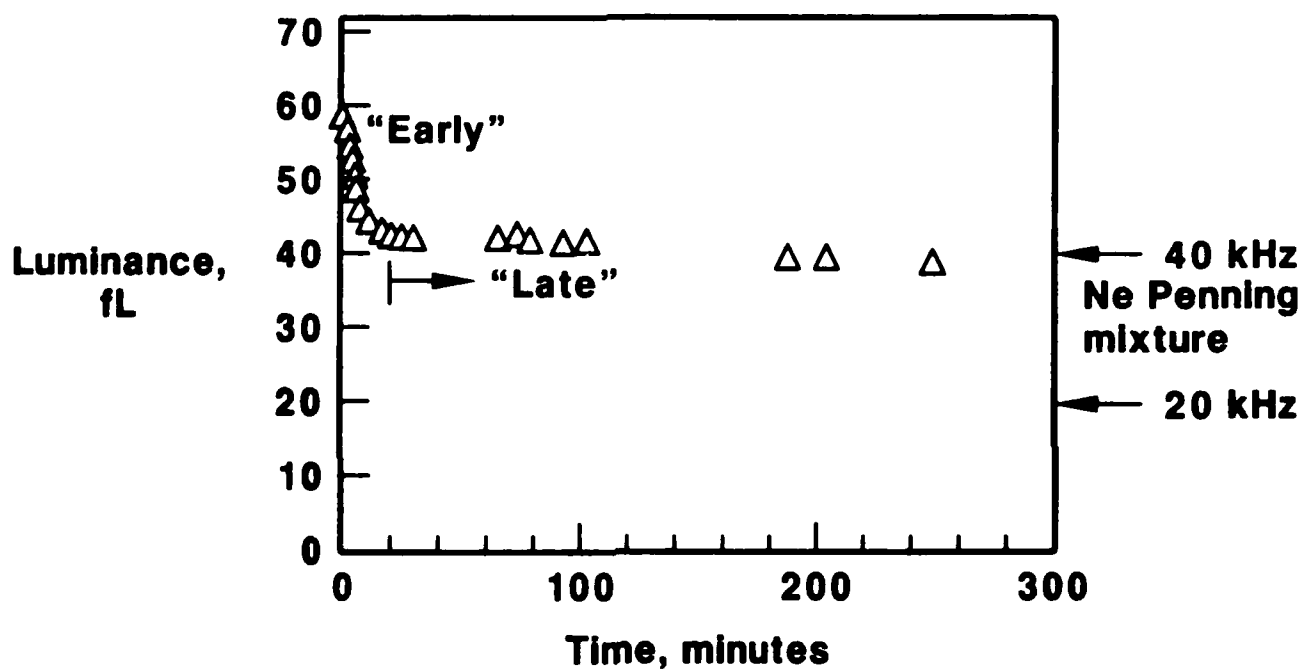
Figure 12.   Luminance temporal decay for a "low conditioned"
panel operating at 200 kHz with a 500 Torr Xe-0.2% O_2
mixture.   Also shown for comparison are the luminance values
of a Ne-Penning mixture. The initial decrease in the "early"
time regime is thought to be the result of gas heating
accompanied by thermal decomposition of the weakly bound XeO
excimer.
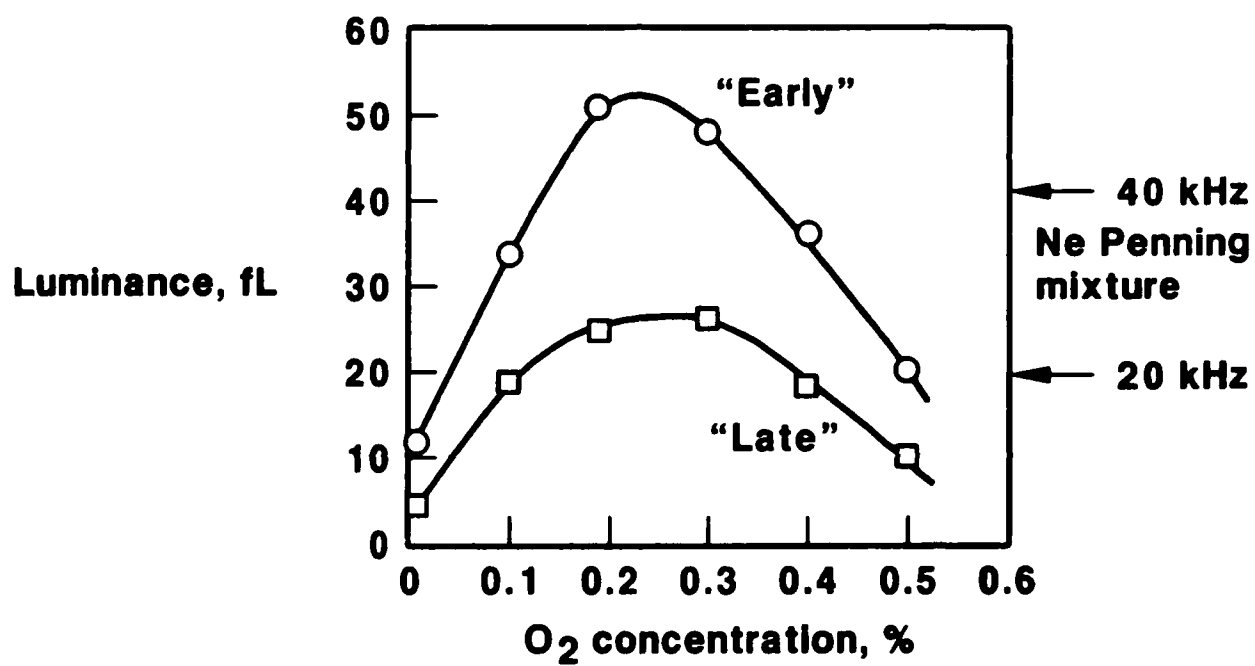
Figure 13. Dependence of luminance on <u>initial</u> O_2 fill concentration for a "low conditioned" panel operating at 200 kHz with a Xe pressure of 500 Torr. The designations "early" and "late" refer to the temporal decay regions indicated in Fig. 12.
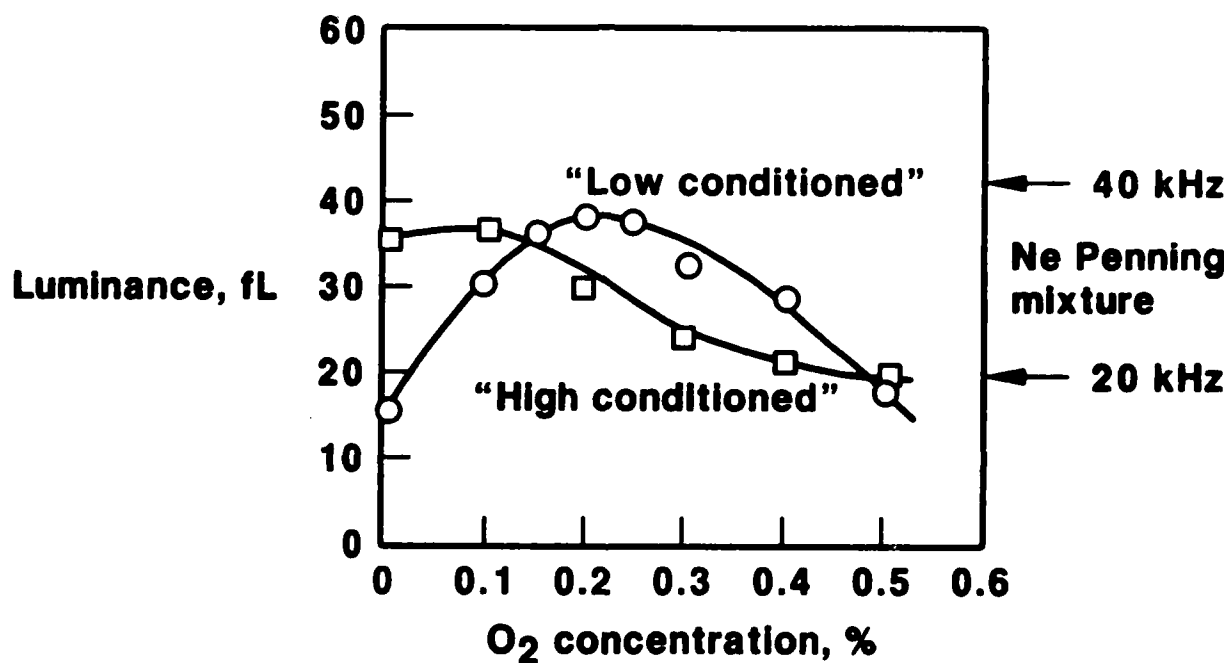
Figure 14. Dependence of luminance on initial O_2 fill fraction for a panel operating at 200 kHz in the "late" regime (Fig. 12). The designations "low" and "high" conditioned refer to the panel preparation technique as described in Section III-B.

appears that an additional history dependent parameter is also at work, although we have not identified the specific cause of the difference exhibited by the data of Figs. 13 and 14.

The luminance data discussed above were obtained at a Xe pressure of 500 Torr. Formation of XeO excimers is a second order pressure dependent-process (Eq. 2c), so one would expect a strong pressure dependence of the luminance under "otherwise similar" conditions. However, totally reproducible experimental conditions are difficult to obtain when history, voltage, and frequency dependent phenomena are occurring. Nonetheless, we have generated many plots of luminance vs. pressure that indicate a pressure-squared dependence, one of which is presented in Fig. 15. These data indicate that luminance values about twice those shown for 500 Torr could be obtained by operating at atmospheric pressure.

Increased luminance can also be obtained by operating at higher frequencies, but above 200 kHz the luminance is no longer linear in operating frequency. Figure 16 shows that above 250 kHz luminance begins to decrease. We believe that the this behavior is most likely the result of heating of the gas so that the XeO excimer molecule becomes less stable (Fig. 8). At the higher frequencies the panel was found to be hot to the touch. Indeed, one test panel was cracked by operating at 500 kHz.

Finally, we have measured the time evolution of light pulses for a variety of conditions. Oscilloscope traces of the emission pulse train are shown in Fig. 17. Adjacent pulses differ in size, leading us to believe that light is emitted in a region very close to each MgO surface. The brighter pulses come from the side of the panel more distant from the viewer (or measurement instrument) which are less affected by electrode blockage. Correlating this observation with voltage polarity shows that the light is emitted close to the electrode that is negative — not a surprising conclusion. Similar behavior was observed for Ne-Penning mixtures, indicating that such behavior is fundamental to the operation of ac plasma panels, independent of gas mixtures.
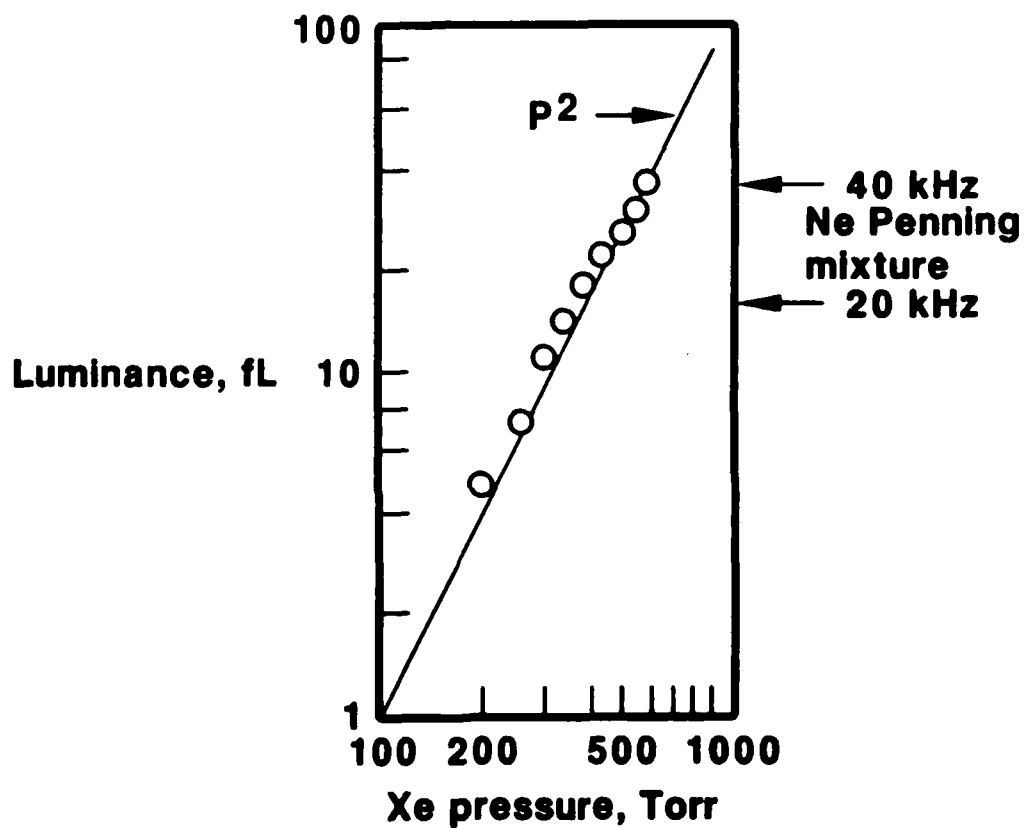
Figure 15. Dependence of luminance on Xe pressure for a Xe-0.4% O_2 mixture operating at 200 kHz. The panel preparation procedure was "low" conditioned and the panel was operating in the "late" temporal regime (Fig. 12).
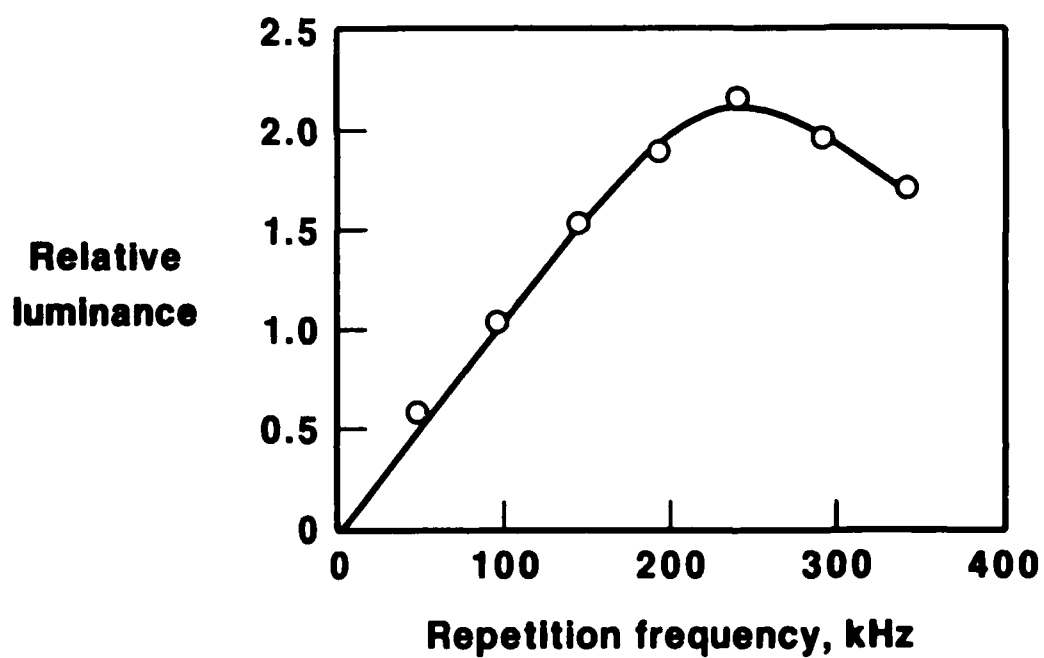
Figure 16. Variation of relative luminance with square wave
repetition frequency for a Xe-0.4% O_2 mixture at 450 Torr.
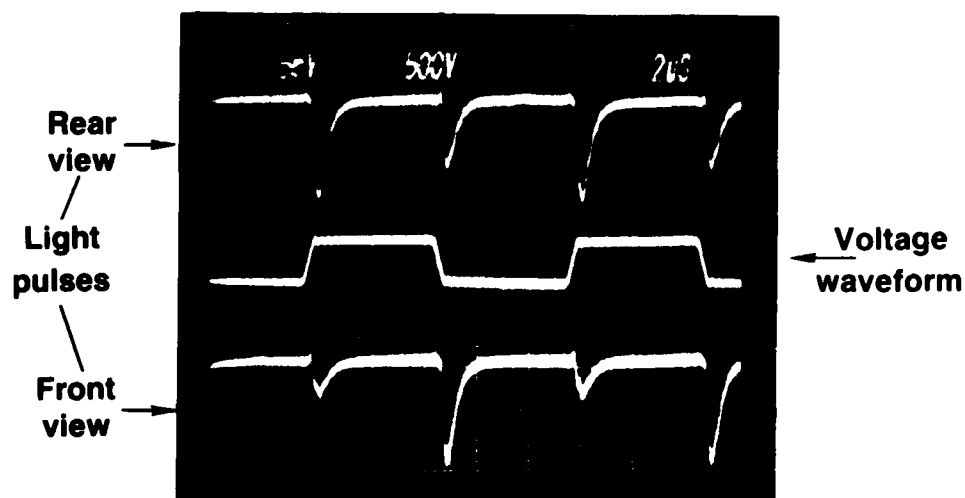
Figure 17. Oscilloscope tracing showing the light emission
pulse train as viewed from the front and rear sides of the
panel. Also shown is the excitation waveform. Positive (up)
voltages correspond to the rear (front) electrodes going
positive (negative). The larger light pulses correspond to
the condition for which the side away from viewer goes
negative.

IV. XeF EXCIMER RESEARCH

We now turn our attention to the XeF excimer which exhibits broadband emission centered at ~ 475 nm, and can be produced in mixtures containing Xe and F_2. Our results for XeF-based excimer mixtures were particularly interesting and encouraging. Using a variety of mixtures we have demonstrated ac plasma panel luminance levels higher than those of the standard Ne-Penning mixture/MgO surface combination excited at the same repetition frequency (50 kHz). Although the experiments carried out to date required operating voltages higher than those of the Ne-Penning/MgO combination, resulting in luminous efficiency levels that are presently 1/3 to 1/10 times lower, the reduced efficiency level is predominantly the result of changes in the MgO electron emitting layer as modified by the presence of F_2, rather than a fundamental limitation of the excimer gas mixture. Indeed, the luminous efficiency levels of Ne-Penning mixtures and XeF excimer mixtures were found to be comparable for the same interior panel surface conditions. Moreover, the XeF based excimer fluorescence exhibited a range of colors continuously variable from pink through white to blue by way of very simple mixture changes. Thus, various colors, and possibly multi-color operation, may be possible within the basic framework of current ac plasma panel technology or reasonable extensions thereof. In the sections to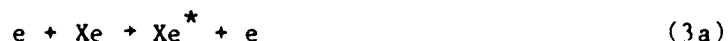 follow the physics of XeF excimer formation is described, along with our experimental results and a discussion of materials issues.

A. XeF Excimer Kinetics

1. XeF Formation

As discussed in Section I, research interest in the physics of excimer molecules has been intense because of their utility as UV/visible laser media. Of this class of molecules, the rare gas halides have received the most attention because of their unusually high formation efficiency when produced in an electric discharge (Ref. 8). The primary rare gas halide transitions are in the UV region (~ 190-350 nm), with the exception of XeF which also exhibits a strong, broadband visible wavelength transition.

In a discharge excited mixture comprised of a rare gas background (RG) and small amounts (< 1%) of Xe and F_2, the two lowest energy ionic states of XeF, B ($\Omega = 1/2$) and C ($\Omega = 3/2$), are produced primarily by way of the following reaction sequence:

$$e + Xe \rightarrow Xe^* + e \tag{3a}$$

$$\rightarrow Xe^+ + 2e \tag{3b}$$

$$RG^* + Xe \rightarrow Xe^* + RG \tag{4a}$$

$$\rightarrow Xe^+ + e + RG \tag{4b}$$

$$Xe^* + F_2 \rightarrow XeF(B,C) + F \tag{5a}$$

$$Xe^+ + F^- + RG \rightarrow XeF(B,C) + RG \tag{5b}$$

Ultraviolet and visible emission results from radiative transitions terminating on the dissociating XeF $X(\Omega = 1/2)$ and A ($\Omega = 3/2$) states, respectively, i.e.,

$$XeF(B) \rightarrow XeF(X) + h\nu, \; 351 \text{ nm} \tag{6a}$$

$$XeF(C) \rightarrow XeF(A) + h\nu, \; 400\text{-}600 \text{ nm} \tag{6b}$$
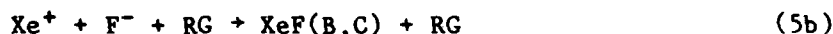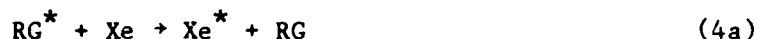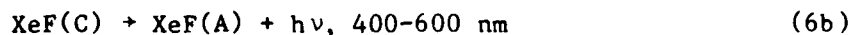
The UV transition is of interest for laser applications (Ref. 8) and will not be discussed further.[†]

2. XeF Vibrational Relaxation

Figure 18 illustrates the XeF C and A potential curves of present interest. Reactions (5a) and (5b) result in the formation of XeF B and C in very high vibrational levels (Refs. 20, 21) as indicated in the figure. Although not shown in Fig. 18, the XeF(B) potential curve is nearly coincident with that of the C state, with the C state lying approximately 0.1 eV lower in energy. For this reason, collisions with background rare gas atoms rapidly transfer energy between the vibrationally excited XeF B and C states, strongly favoring population buildup of XeF(C). Vibrational relaxation of XeF B and C, also the result of the collisions with the background gas, occurs simultaneously with the XeF(C) population buildup due to B-C mixing (Refs. 20, 21). For the high pressures typical of laser applications (p > 2 atm), nearly complete vibrational relaxation occurs in a time much less than the 100 nsec radiative lifetime of XeF(C). In that case, a room temperature Boltzmann

---

[†]The 351 nm wavelength of the XeF(B→X) transition is significantly longer than the rare gas dimer emission (< 200 nm) often used to excite phosphors, and may be well suited for that application, either alone or in conjunction with the visible XeF(C→A) transition.

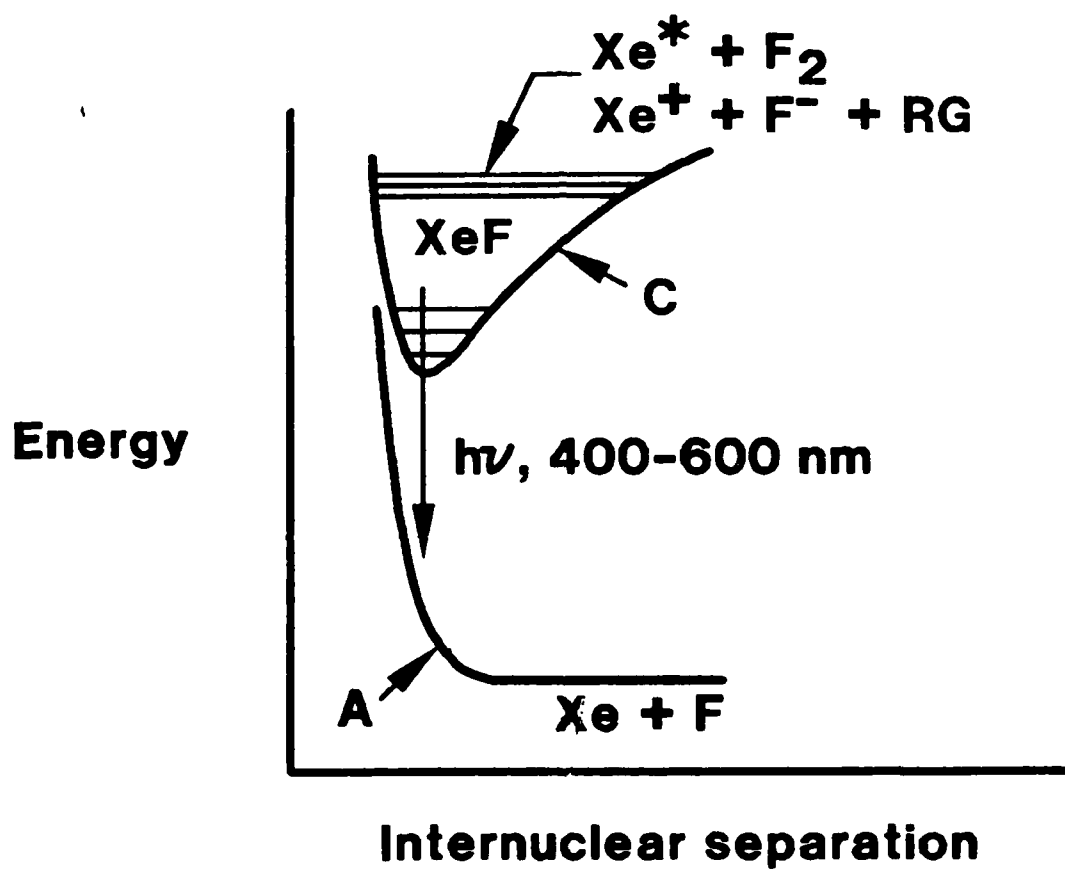Figure 18. Potential energy diagram illustrating XeF
$C(\Omega = 3/2)$ and $A(\Omega = 3/2)$ states. Reactions 5a and 5b
resulting in the formation of XeF(C) in high vibrational
levels are indicated.

vibrational distribution is established prior to XeF(C→A) radiative decay, and a broadband C→A emission spectrum centered at 475 nm results, having a spectral width of ~ 70 nm (FWHM) (Refs. 20-22). However, for background gas pressures **below** one atmosphere, the pressure range of interest for displays, the time required for XeF(C) vibrational relaxation is approximately the same as the 100 nsec spontaneous decay time, with the result that the two processes occur simultaneously. Because higher vibrational levels are then involved in the C→A radiative process, and since the terminal XeF(A) state passes close to XeF(C) at reduced internuclear separation (Fig. 18), both shorter and longer wavelength emission results. The broadening effect on the visible spectrum when high XeF(C) vibrational levels contribute to the C→A fluorescence (i.e., $T_v \gg 300$ °K) is illustrated in Fig. 19.

Vibrational relaxation of the XeF B and C state manifolds has been studied extensively (Refs. 20, 21), and it has been found that for background gas pressures less than atmospheric, Ne and He are relatively ineffective at relaxing the XeF(C) vibrational levels. However, Ar and Kr are very much more effective, particularly Kr. Since the presence of Ar and Kr is also compatible with efficient XeF formation (Ref. 23), this indicates that the degree of XeF(C) vibrational relaxation (i.e., T_v), can be controlled by judicious selection of rare gas background constituents. Thus, XeF(C→A) spectral properties and therefore display color can be varied by simply changing the gas mixture.

B. Procedures for XeF Experiments

In addition to the general procedures described in Secs. II and III, for the XeF research it was necessary to account for the high chemical reactivity of F_2. Prior to experimentation with each test panel, the interior surface of the panel and all vacuum system parts exposed to excimer mixtures were passivated for several **days** by filling the system with several hundred Torr of a He-5% F_2 mixture which was flushed and changed frequently. Most of the experimental results to be described subsequently were obtained using a conventional panel produced with an interior surface of MgO in the display region. We believe that the F_2 passivation procedure converted a few **monolayers** of the MgO surface to MgF_2 as illustrated in Fig. 4. Regarding the effect of F_2 passivation on other interior materials, such as the glass edge seal and the connection to the gas handling system, subsequent experimentation revealed that the passivation was not complete. However, temporal changes in electrical/optical properties, implying a change in F_2 concentration, were not observed until after several hours of con*inuous operation, a circumstance providing more than enough time for careful, systematic evaluation of XeF display properties. Considering the nature of the experimental arrangement and the fact that panel interior materials were not designed to be
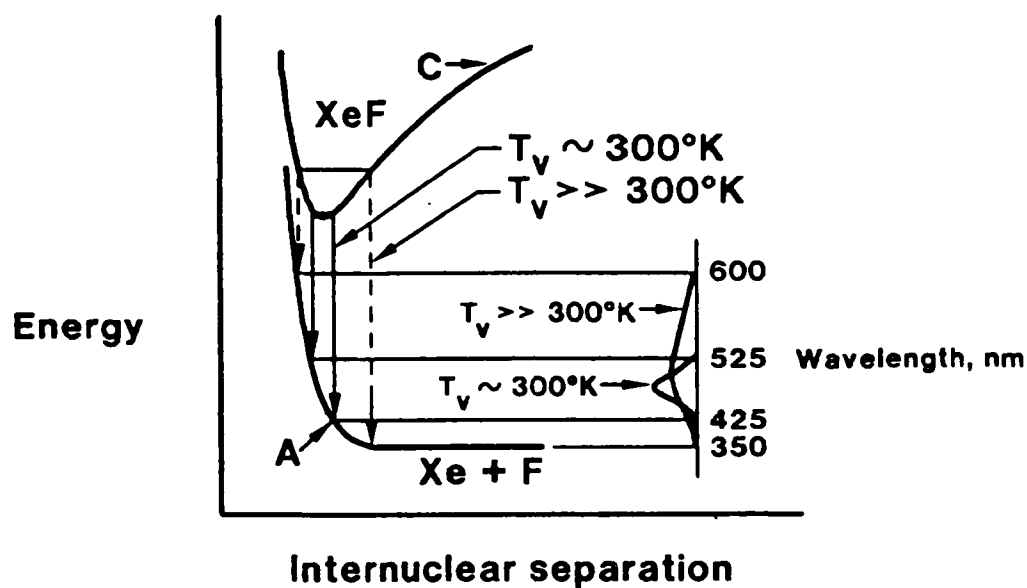
Figure 19. Illustration of XeF(C→A) emission from low and high vibrational levels, and the broadening effect of the latter on the C→A spectral distribution.

F_2 compatible, we consider the observed degree of materials/mixture compatibility to be encouraging, a topic to be discussed in more detail in subsequent sections.

C. Results

1. Emission Properties

After completion of the passivation procedure described above, the test panel was filled with a Ne-0.2% Xe-Penning mixture at a pressure of 500 Torr. The orange color was found to be typical of the standard reference condition for this panel **prior** to passivation. However, the luminance was about 1.8 times higher and the pixel resolution was quite poor (Fig. 5). In addition, the firing voltage increased by more than a factor of two, reflecting the change in the electron emitting internal surface from MgO to MgF_2.

a) XeF Base Mixture: By increasing the Xe concentration from the ~ 0.2% typical of the Penning mixture to a few Torr, and after the addition of approximately 1 Torr F_2, the color changed from orange to pink with an increase of luminance level. For example, for a mixture comprised of Ne+0.6%Xe+0.2%F_2 at 500 torr the luminance level was approximately twice as high as that of the standard Ne-Penning mixture/MgO surface combination operating at the **same** repetition rate (i.e., 50 kHz). Although the luminance was not unduly sensitive to the specific Xe and F_2 concentrations, the maximum luminance observed occurred for Xe and F_2 concentrations of about 1% and 0.2% respectively. Figure 20a shows the spectrum for this XeF mixture, which will be referred to in all subsequent discussion as the "base mixture". The addition of F_2 had very little effect on the Ne line emission compared with that of a Ne-Penning/MgO combination, resulting in only a 20 percent decrease in luminance. However, in addition to the Ne emission, there appeared the continuous XeF(C→A) excimer emission spanning most of the visible region. The XeF(C→A) spectral shape of Fig. 20a is typical of the emission from many XeF(C) vibrational levels (i.e., T_V >> 300 °K, Fig. 19). The combination of the Ne reddish-orange color with the nearly "white" XeF(C→A) emission results in the observed pink emission at a high luminance level.

b) Ar and Kr Addition: As explained previously, Ar and Kr are known to be much more effective than Ne at relaxing XeF(C) vibrational levels. Addition of 25-75 torr of Ar to the Ne-Xe-F_2 mixture of Fig. 20a was found to diminish the luminance somewhat and to change the color from pink to "white", often with either a slight pink or blue tint depending on the specific Ar concentration. Presented in Fig. 20b is a representative spectrum for a mixture containing Ar. Clearly the intensity of the Ne line emission was reduced significantly in this case, and the shape of the C→A XeF emission was
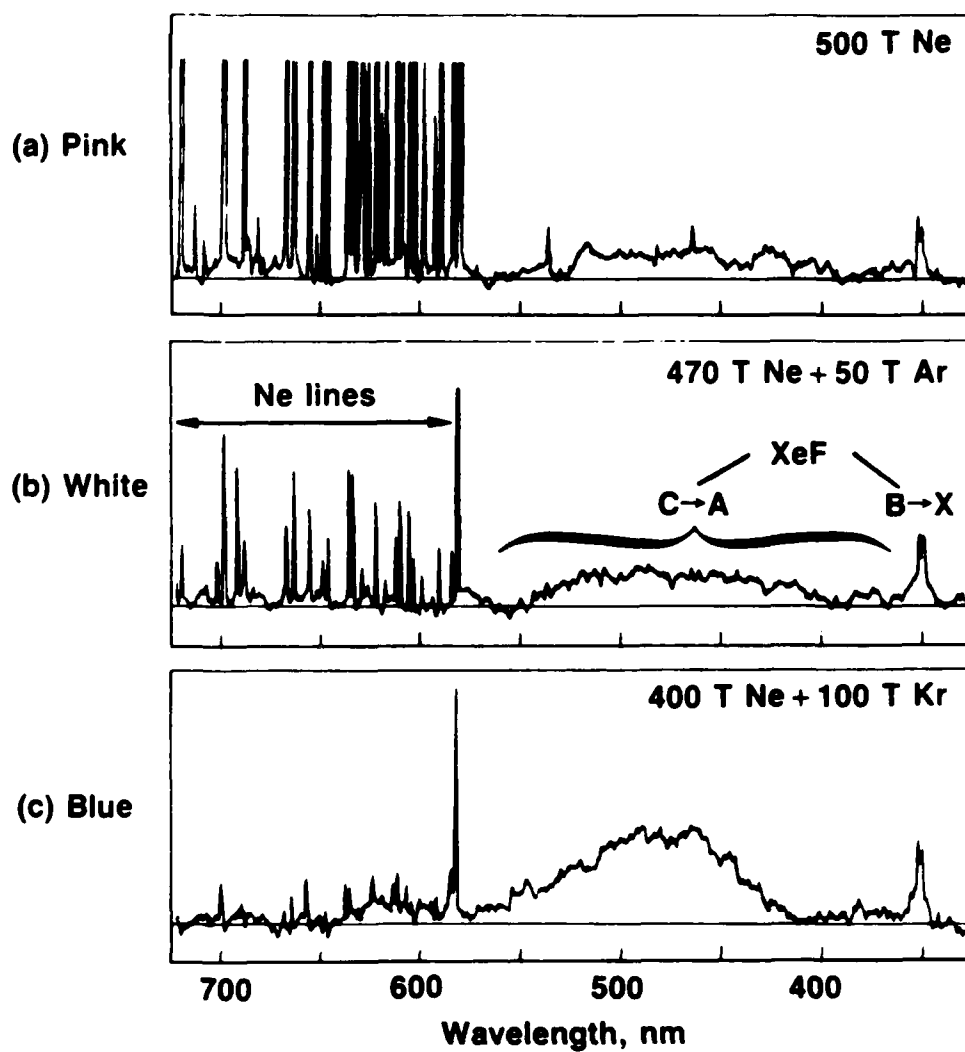
Figure 20. Measured spectral properties for the following 500 Torr mixtures: (a) Ne, 3 Torr Xe, and 1 Torr F_2 (pink); (b) Ne, 3 Torr Xe, 1 Torr F_2 and 500 Torr Ar ("white"); (c) Ne, 3 Torr Xe, 1 Torr F_2 and 100 Torr Kr (blue).

35

better defined, exhibiting a broad maximum centered at about 475 nm. With the addition of Kr in place of Ar, this trend was further accentuated. Figure 20c shows that with 100 Torr Kr added to a Ne-Xe-F_2 base mixture, the Ne line emission was quenched almost completely and the XeF(C→A) emission exhibited the shape typical of a nearly room temperature Boltzmann distribution (Refs. 20-22). In this case, the emission appeared blue and the measured luminance was essentially the same as that of the Ne-Penning mixture/MgO surface combination operating at the same repetition frequency.

The data of Fig. 20 show that the spectral shape, and therefore the color, of the XeF(C→A) emission can be changed by controlling the effective XeF(C) vibrational temperature, and by combining XeF(C→A) emission with Ne line emission. The chromaticity diagram of Fig. 21 illustrates the range of colors that have been observed and the approximate path through the color regions corresponding to the combined suppression of Ne line radiation and vibrational relaxation of XeF(C), both of which occurr in response to addition of either Ar or Kr. Measured color coordinates for the mixtures of Fig. 20 are labeled a, b, c for the conditions resulting in pink, white, and blue emission, respectively.

2. Electrical and Optical Properties

As mentioned previously, F_2 passivation of the initial MgO panel surface resulted in an increase in the firing voltage of the Ne-Penning mixture from ~ 100 V to 250 V; the voltage margin was ~ 25 V for the initial MgO surface and ~ 40 V for the passivated surface. For typical Ne-Xe-F_2 mixtures the firing voltage increased to ~ 300 V but the extinction voltage did not change, with the result that the memory margin increased significantly to ~ 80-90 V. Addition of either Ar or Kr to the Ne-Xe-F_2 mixture further increased both the firing voltage and the margin, with little change in the extinction voltage.

Presented in Fig. 22 are the pixel firing and extinction voltages as a function of pressure for a representative mixture containing Kr. The firing and extinction voltages and the margin exhibited a very weak dependence on pressure in the 200-700 torr range for all XeF mixtures examined. Additionally, Fig. 23 shows that the voltage margin exhibited no significant dependence on repetition frequency.

Figure 24 show the luminance dependence on repetition frequency for our "base mixture". There is clearly some nonlinearity above 200 kHz. However, the luminance in the 50 to 100 kHz range is two or more times that of the Penning/MgO combination at 50 kHz, a value which is close to the upper operating limit for conventional panels.
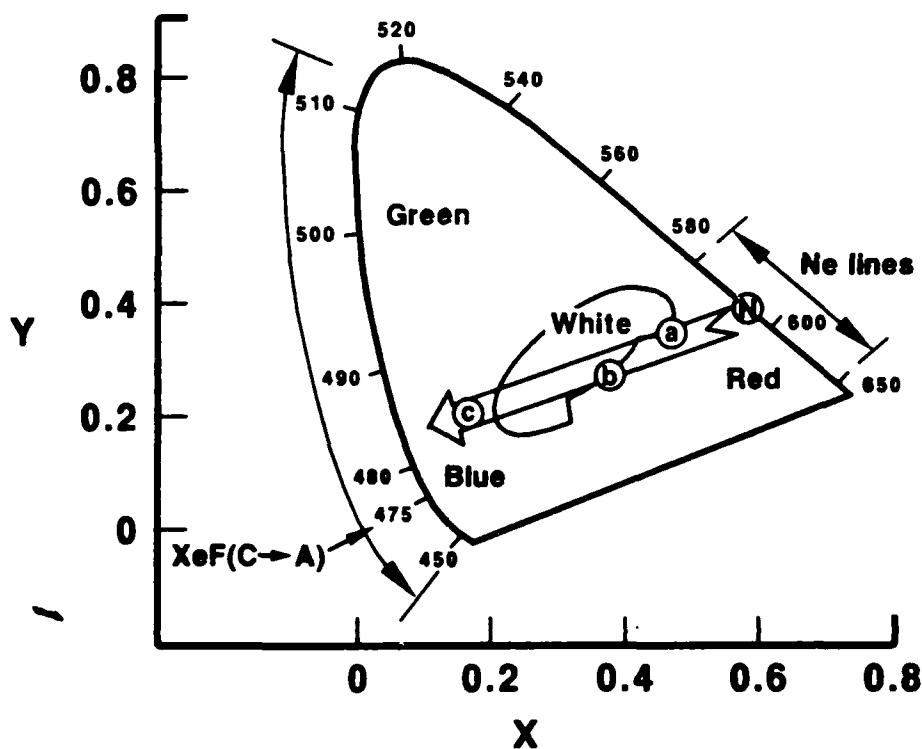
Figure 21. Adaptation of the 1931 CIE chromaticity diagram illustrating the range of colors observed from XeF-based display mixtures. The shape and location of the arrow are intended to show the approximate path through the various color regions in response to the addition of either Ar or Kr to our XeF "base" mixture. The letter N refers to a Ne-Penning mixture and a, b and c refer to the observed colors corresponding to the spectra of Fig. 20. The spectral width (FWHM) corresponding to a near room temperature XeF(C) vibrational distribution (blue emission) is also indicated.
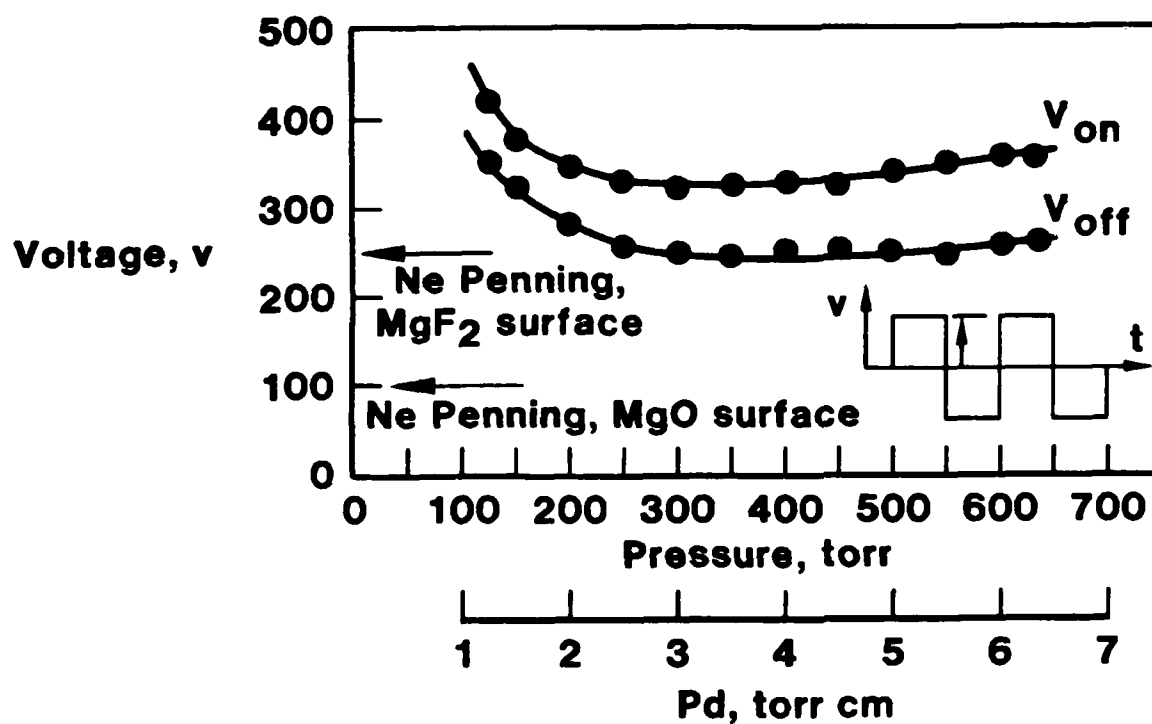
Figure 22. Firing (V_{on}) and extinction (V_{off}) voltages at a square wave repetition frequency of 50 kHz for a mixture comprised of Ne, 0.6% Xe, 0.2% F_2 and 5% Kr. For this mixture the emission was "white" at 500 Torr.
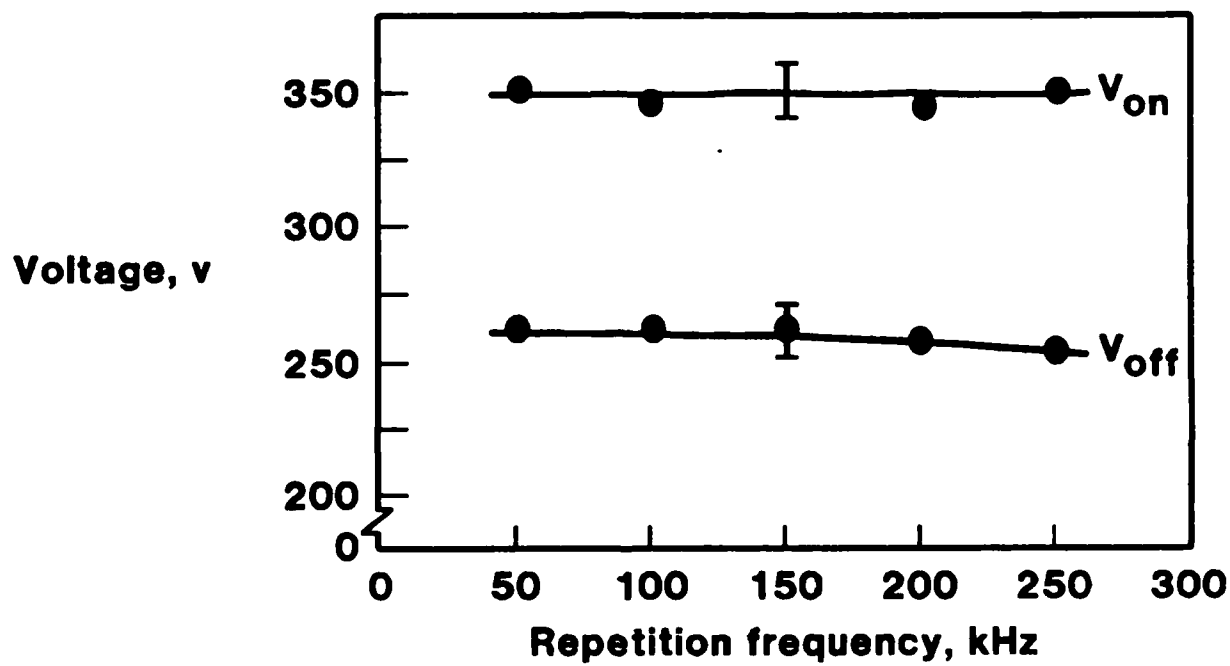
Figure 23. Variation of firing (V_{on}) and extinction (V_{off})
voltages with repetition frequency corresponding to the
mixture of Fig. 22 at a pressure of 500 Torr.
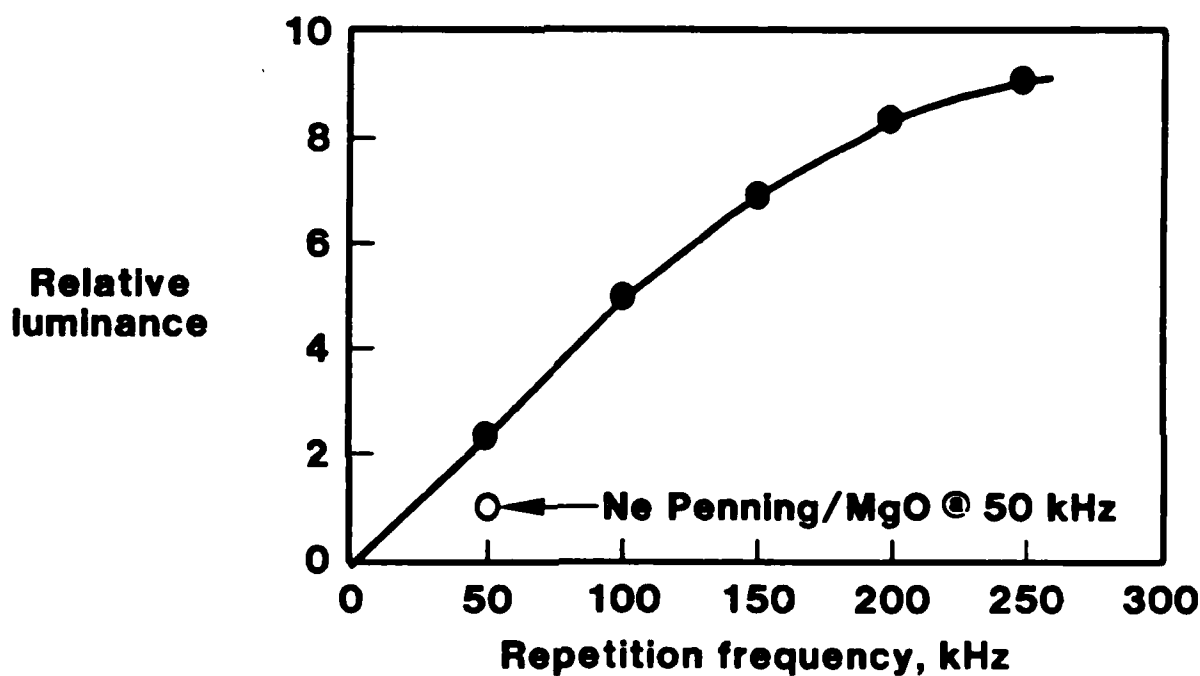
Figure 24. Variation of the relative luminance with square
wave repetition frequency for a representative (but not
optimized) mixture comprised of Ne, 3 Torr Xe and 1 Torr F_2
at a total pressure of 500 Torr. For these conditions the
pixel color was pink. The data points were normalized with
respect to the luminance measured at 50 kHz for the standard
Ne-Penning mixture/MgO surface combination of our reference
panel.

Electrical and optical properties of representative (but not optimized) XeF-based mixtures are summarized in Table I, which also presents the comparative characteristics of our Ne-Penning/MgO reference panel, along with the properties of a Ne-Penning/MgF$_2$ panel. In the table, the designation "poor" resolution refers to near overlap of lighted regions of adjacent pixels, "good" refers to a discharge small compared with pixel spacing, with "fair" referring to an intermediate condition, as illustrated in Fig. 5.

3. Durability Measurements

Long-term durability remains a key issue. We now are optimistic that a saturated fluorine compound (such as MgF$_2$) provides an adequate inner surface within the discharge region, provided that there are no other "sinks" for the F$_2$ (or F) that will result in the gradual consumption of F$_2$ over time. To evaluate F$_2$ lifetime, it was found that observation of the temporal change of the 1931 CIE x,y color coordinates was the most reliable and convenient technique for measuring decrease in the F$_2$ level. In this work an initial XeF "base" mixture was used resulting in pink emission (x $\cong$ 0.42, y $\cong$ 0.35), Figs. 20a and 21. The gradual temporal evolution of the x,y coordinates was carefully monitored until the emission became orange (x $\cong$ 0.60, y $\cong$ 0.39), a condition indicative of the complete disappearance of F$_2$.

Measurements were carried out using two modes of operation. The "OFF mode" corresponded to the panel left off most of the time, and lighted (in a 1" x 1" test patch) only for the time required to measure x and y, i.e., < 1 min. This procedure provided a measure of the loss of F$_2$ due to sinks other than the discharge surface (e.g., edge seals), assuming that the interior surface is well passivated. The procedure used for the "ON mode" was similar, with the important exception that the test patch remained lighted throughout the entire experiment so as to reveal additional effects at the surface exposed to the discharge.

Three panels were evaluated using these procedures: an F$_2$-passivated MgO panel, and two specially fabricated panels having inner layers of Al$_2$O$_3$, and MgF$_2$, respectively. The latter two panels were custom-made for UTRC by Electro-Plasma, Inc. The E.P.I. panels were constructed with a coated "dam" (i.e., either Al$_2$O$_3$ or MgF$_2$) made of spacer material surrounding about 90% of the peripheral inner region. Except for a small gap to the pumpout port, the dam served to shield the panel edge seal material from F$_2$. Al$_2$O$_3$ and MgF$_2$ were selected as inner layer materials based on the experience of the excimer laser community (Ref. 24) showing that Al$_2$O$_3$ and MgF$_2$ films offer good protection of optical elements continuously exposed to F$_2$-containing gas mixtures similar to those of the present work. Additionally, Al$_2$O$_3$ was expected to have electron emission characteristics generally similar to those of MgO (Ref. 25).

TABLE I
Typical properties of XeF-based display mixtures

Mixture	Relative lumi-nance[*]	Mid-margin sustain voltage	Voltage margin	Color	CIE 1931 x,y	Resolu-tion	Relative luminous efficiency[*]
Ne Penning MgO	1	100 V	25 V	Orange	0.60,0.39	Good	1
Ne Penning MgF_2	1.8	240	40	Orange	0.60,0.39	Poor	0.3
XeF base	2.1	260	90	Pink	0.47,0.35	Fair	0.3
Base + 5% Kr	1.4	300	90	Pinkish white	0.38,0.24	Fair	0.15
Base + 10% Kr	1.1	300	95	Bluish white	0.33,0.21	Good	0.12
Base + 20% Kr	1.0	315	110	Blue	0.17,0.22	Good	0.1

[*]Relative luminance and relative luminous efficiency are measured relative to a standard test panel (Ne Penning mixture/MgO surface) operating at 50 kHz. The XeF Base mixture is comprised of Ne - 3 T Xe - 1 T F_2 at a total pressure of 500 Torr; the Ne partial pressure is reduced as Kr is added.

All of the measurements exhibited time dependent color coordinates x,y which followed an almost linear path from the initial pink emission to orange, i.e., complete F_2 loss. Therefore, it is convenient to use normalized plots of percentage change in the x,y coordinates as they vary with operating time. A plot summarizing the results presented in this manner is shown in Fig. 25. Qualitatively, the time-dependence of the "OFF" mode is not radically different for the three panels, suggesting that the F_2-sinks external to the interior discharge surface region are similar in all three, and that the "dam" shielding the edge seal had relatively little effect. However, the temporal decay profiles for the panels operating continuously ("ON") were found to be significantly different. The F_2-passivated MgF_2 panel decays more rapidly in the ON mode than in the OFF mode (Fig. 25a), suggesting that operating the discharge is converting some MgO to MgF_2, with a corresponding loss of F_2. Additionally, discharge operation results in the generation of F atoms (Eq. 5a) which may have a higher and/or different reactivity with the passivated surface than that of F_2 molecules.

The difference between "ON" and "OFF" mode operation was dramatically different for the Al_2O_3 panel (Fig. 25b). Although Al_2O_3 has been found to be an excellent protective film for laser applications (Ref. 24), loss of F_2 was practically instantaneous when the Al_2O_3 coated panel was operated continuously. This rather surprising result suggests either a very high reactivity of Al_2O_3 with F atoms, or discharge induced surface damage. Another possibility that cannot be ruled out is that the Al_2O_3 film was flawed. The latter explanation seems unlikely, since Al_2O_3 is often used for purposes such as this, and E.P.I. has experience depositing high quality Al_2O_3 for plasma panel applications. In any case, our Al_2O_3 test panel was found to be entirely unsatisfactory.

The situation was found to be substantially more encouraging when the MgF_2 panel was tested (Fig. 25c). Initially, the ON mode performance was not very different from the OFF mode for the MgF_2 coated panel. However, after a number of runs some difference was observed, and a clearly visible deposit appeared at the location of the discharge patch. We believe this patch to be pure Mg left after the F_2 sputtered from the patch by the discharge was gradually consumed at some external site(s). In view of our earlier results with Xe-O_2/XeO excimer mixtures using an MgO panel, ("high/low conditioning" (Section III-B)), it is not surprising that there is exchange of F_2 between the gas and the MgF_2 surface. What appears to be different in this case is that the F_2 can be consumed while the excess O_2 in the XeO case could return to th MgO when the discharge was extinguished That is, the O_2/MgO reactions are nearly fully reversible while the F_2/MgF_2 reactions are not. Nonetheless, our experience with the MgF_2 panel has to be viewed as encouraging, indicating that MgF_2 may be an acceptable long life interior coating, provided that means of completely passivating all internal surfaces (including the pumpout port and edge seal) can be devised.
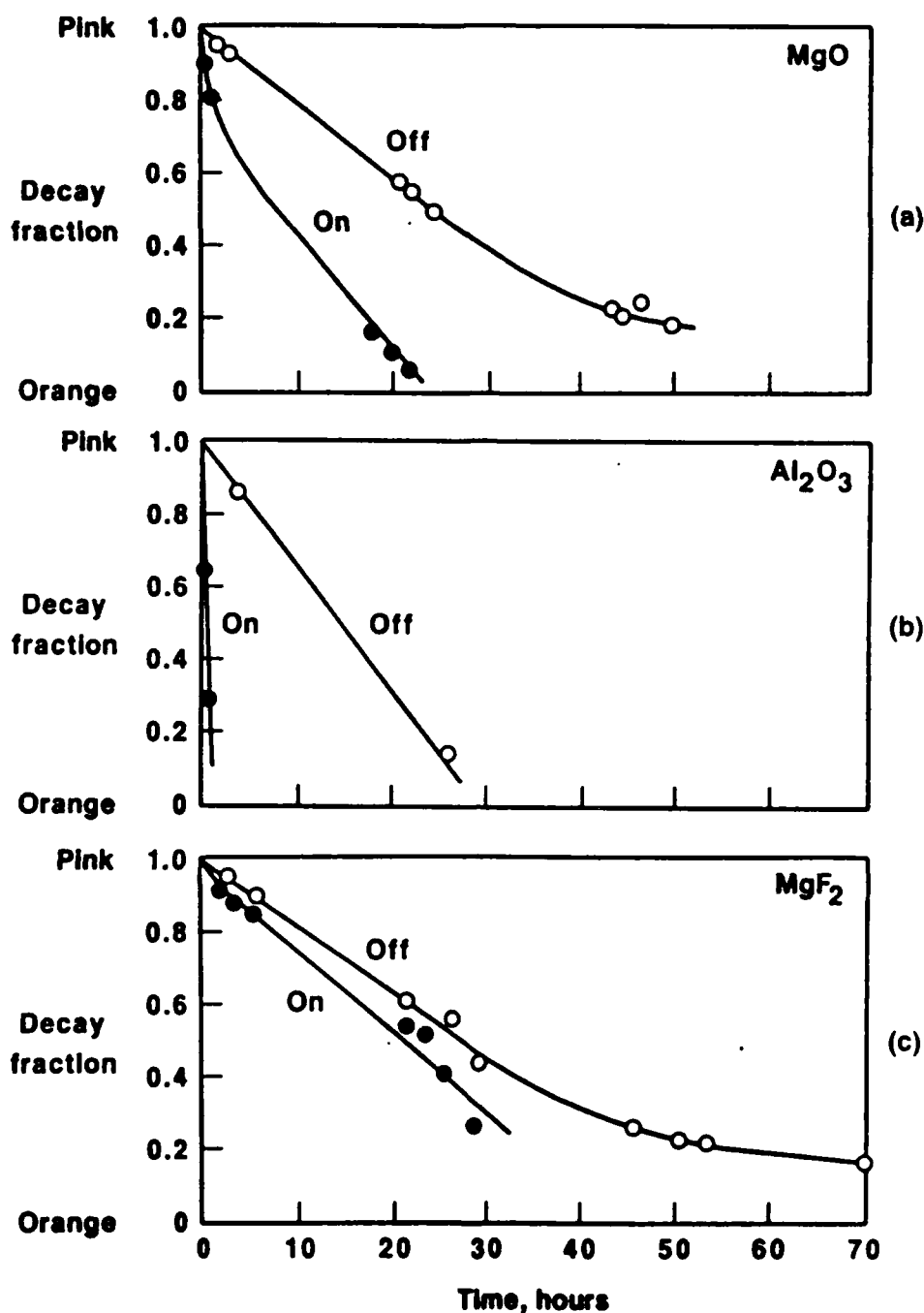
Figure 25. Temporal evolution of C.I.E. 1931 x,y coordinates
for a mixture initially comprised of 500 Torr Ne, 3 Torr Xe
and 1 Torr F_2, operating at 50 kHz. These data were obtained
using three different panels: an F_2-passivated MgO panel (a);
a panel fabricated with an Al_2O_3 inner surface (b); and a
panel fabricated with an MgF_2 inner surface (c). As
described in the text, the designations "On" and "Off" refer
to whether or not the panel was operating throughout the
entire test period or just at the time the chromaticity
coordinates were measured.

V. SUMMARY AND DISCUSSION

A. Excimer Concept

Since the time ac plasma panels became practical in the 1960's, workers have been searching for gas mixtures capable of producing colors other than the well known neon-orange characteristic of Ne-Penning mixtures. The history of this effort is reviewed briefly in Section I. In this research we have been investigating an entirely different alternative to the excitation of stable gaseous species which subsequently fluoresce. Based on our background in excimer laser technology, we have carried out an investigation of the feasibility of utilizing visible excimer molecule fluorescence for display purposes. Because large area ac plasma panels based on the Owens-Illinois Digivue™ design (Ref. 1) have become a well developed industry standard, we have concentrated our research on plasma panels of that type. It should be recognized, however, that restriction of our research to that specific panel design represents an important limiting factor in the evaluation of the viability of the excimer display concept.

After an initial analytical and experimental evaluation of potential excimer candidates, we focused our attention on two: XeO (green) and XeF (blue-green). No doubt, the single most significant outcome of our research was the demonstration that visible fluorescence from these excimers can be generated at a luminance level equivalent to that of the standard Ne-Penning mixture, using a unmodified ac plasma panel of conventional design. At the beginning of the program, it was by no means certain that such would be the case.

B. XeO

The XeO excimer is produced in mixtures comprised of Xe and O_2. Both Xe and O_2 are species that should be compatible with conventional plasma panel materials, and that was felt to be a distinct advantage. Moreover, Xe at pressures of a few hundred Torr had been used in the past as a source of UV in research directed toward evaluation of phosphor excitation (Sec. I). Thus, it was felt that the electrical properties of Xe-O_2 plasma panels would be satisfactory, although a higher operating voltage was anticipated.

After overcoming a considerable amount of experimental difficulty arising from the complex interchange between surface and gas phase O_2, XeO green-band luminance levels comparable to those of Ne-Penning mixtures were obtained, albeit at a pulse repetition frequency approximately five times that of the Penning mixture (Figs. 12-15). The relatively large O_2 fraction required for XeO formation, combined with the complex gas-surface chemistry referred to

previously, apparently had a very significant adverse affect on the electron emission characteristic of the MgO surface, as manifested by a undesirable voltage-pressure dependence (Fig. 11).

Although the XeO luminance was acceptable, the high repetition rate and high voltage level required are indicative of a luminous efficiency very much lower than that of Penning mixtures. We have learned that there are fundamental reasons for the low efficiency: $O(^1S)$, the precursor of XeO, is produced with a low ($\sim 1\%$) efficiency in electric discharges, and $O_2(a^1\Delta_g)$, the primary collisional deactivator of $O(^1S)$, is produced so efficiently that its fractional concentration reaches a level on the order of 10-20% of the original O_2 fill pressure. These two factors combined have a severe adverse effect on XeO luminous efficiency. There is no doubt that if a more efficient source (other than O_2) of discharge excited $O(^1S)$ could be found, or if kinetic or surface means of reducing the $O_2(a^1\Delta_g)$ concentration could be devised, both the absolute luminance and luminous efficiency of XeO emission could be significantly increased. Solutions to these problems represent a formidable task, however.

Finally, it should again be pointed out that XeO luminance increases as the square of the pressure (Fig. 15), while the power consumption varies somewhat less than linearly with pressure. Therefore, significantly higher luminance and luminous efficiency levels would be possible if operation at pressures above atmospheric were practical. For example, the trend of Fig. 15 indicates that operation at ~ 1.5 atm would result in XeO luminance approximately equal to that of the Penning mixture, with both operating at the **same** repetition frequency. Reduction of the panel gap spacing by $\sim 50\%$ would result in about the same voltage levels. Consideration of such factors, along with the exceptional match of XeO fluorescence with the response of the eye, suggests that XeO may have potential for a limited number of display applications for which green emission is required. However, it seems safe to conclude that an excitation structure significantly different from the ac plasma panel would be required.

C. XeF

The XeF excimer is produced in mixtures containing Xe and F_2, and we knew at the outset that XeF production would be very much more efficient than XeO formation, provided F_2 at the required concentrations could be retained in the gas phase. In fact, we found working with F_2-containing mixtures to be far less of a problem than expected, at least as far as short time ($\sim$ hours) operation is concerned. Moreover, some unique and unexpected performance features associated with XeF mixtures were discovered.

A variety of colors ranging from pink through "white" to blue have been produced in an ac plasma panel by combining neon line emission with very broadband XeF excimer emission (Fig. 21). A specific color or white can be obtained simply by changing the relative proportions of the rare gas mixture constituents. Moreover, although no attempt was made to optimize the concentrations of mixture constituents, the luminance levels of XeF-based mixtures were found to be at least equal to, and in some cases significantly higher than those produced by the Ne-Penning mixture/MgO surface combination of our reference panel operated at the same repetition frequency.

The ability of our XeF mixtures to produce emission over a large portion of the visible spectrum suggests that additional flexibility can be obtained using various filters. Also, color ac plasma panel displays without the use of phosphors may be a possibility by combining the broadband visible emission of XeF-based mixtures with some sort of fast optical switching device, or by using an array of micro-filters to form a pixel.

The qualitative dependence of ac panel ignition and extinction voltages on pd and the voltage memory margin are favorable for XeF mixtures (Fig. 22). However, the voltage level is approximately three times higher than that of the standard Ne-Penning/MgO combination, due primarily to the nature of the fluoride inner surface. Thus, the luminance efficiency is lower than that of the standard panel. This factor is partially offset for mixtures having a luminance that is higher than that of the standard system, thereby permitting operation at lower repetition frequency. Since further increases in luminance are likely as optimum XeF mixtures are identified, an improvement in luminous efficiency seems certain. Nonetheless, the higher operating voltage is disadvantageous, and means to reduce the voltage level are definitely worthy of consideration.

Without doubt, the key issue that will determine the viability of XeF-based plasma displays is device lifetime using mixtures containing F_2, whether using a panel of the Digivue™ design or some other structure. However, this problem is probably not as formidable as it might seem at first, an observation supported by our initial experience with an F_2 passivated ac panel of conventional construction, and most recently with a panel constructed with an MgF_2 inner layer. During the last few years extensive research has been carried out by the laser community to identify optical and discharge materials that do not react with F_2, or can be thoroughly passivated against F_2 attack (Ref. 24). In certain rare gas fluoride laser applications very long device lifetime is as important as in the case for displays, a problem that is greatly complicated by the fact that in lasers numerous materials are usually in contact with F_2. Additionally, laser system configuration is exceptionally complex compared with typical display envelopes. Indeed ac plasma displays of the type used in this investigation feature very simple inner structures in

which few different materials are actually in contact with the gas, and only one is in contact with the discharge. It seems reasonable that with minor changes in design or fabrication, only a single material need be in contact with F_2.

Although the comprehensive investigation required to address and solve these materials problems is beyond the scope of the present investigation, we conclude that XeF does have potential for development as a plasma display medium. In order to justify the additional effort and expense required to capitalize on X_2F properties, it seems likely that a concept must emerge that has well recognized potential for a full color (or multi-color) display.

REFERENCES

1. L. F. Weber, "Plasma Displays", in Flat Panel Displays and CRTs, L. E. Tannas, Jr., Ed., New York: Van Nostrand Reinhold, 1985, Chap. 10.

2. O. Sahni, C. Lanza and W. E. Howard, J. Appl. Phys., Vol. 49, pp. 2365-2379, 1978.

3. W. L. Nighan, IEEE Trans. Electron Devices, Vol. ED-28, pp. 625-630, 1981.

4. W. E. Ahearn and O. Sahni, "The Dependence of the Spectral and Electrical Properties of AC Plasma Panels on the Choice and Purity of the Gas Mixture," in 1978 SID International Symp. Dig. Tech. Papers, pp. 44-45, 1978.

5. O. Sahni, "Blue Color AC Plasma Panel," in 1980 SID International Symp. Dig. Tech. Papers, pp. 82-83, 1980.

6. W. L. Nighan and C. M Ferrar, Appl. Phys. Lett., Vol. 40, pp. 223-225, 1982.

7. C. M. Ferrar and W. L. Nighan, IEEE Trans. Electron Devices, Vol. ED-30, pp. 439-443, 1983.

8. Topics in Applied Physics, Vol. 30, "Excimer Lasers", C. K. Rhodes, Ed., New York: Springer-Verlag, 1979.

9. G. Black, R. L. Sharpless and T. G. Slanger, J. Chem. Phys., Vol. 63, p. 4546, 1975.

10. K. H. Welge and R. Atkinson, J. Chem. Phys., Vol. 64, p. 531, 1975.

11. T. H. Dunning and P. J. Hay, J. Chem. Phys., Vol. 66, p. 3767, 1977.

12. V. S. Zuev, L. D. Mikheev and I. V. Pogorel'skil, Sov. J. Quantum Electron., Vol. 9, p. 884, 1979.

13. J. Balamuta and M. F. Golde, J. Chem. Phys., Vol. 76, p. 2430, 1982; also J. Phys. Chem., in press.

14. G. Black and T. G. Slanger, J. Chem. Phys., Vol. 74, p. 6517, 1981.

15. S. J. Arnold, E. A. Ogryzlo and H. Witzke, J. Chem. Phys., Vol. 40, p. 1769, 1964.

16. S. N. Foner and R. L. Hudson, J. Chem. Phys., Vol. 25, p. 601, 1956.

17. T. G. Slanger and G. Black, Geophys. Res. Lett., Vol. 8, p. 535, 1981.

18. T. G. Slanger and G. Black, J. Chem. Phys., vol. 75, p. 2247, 1981.

19. R. D. Kenner and E. A. Ogryzlo, J. Photochem., Vol. 18, p. 379, 1982.

20. H. C. Brashear, Jr. and D. W. Setser, J. Chem. Phys., Vol. 76, pp. 4932-4946, 1982.

21. Y. C. Yu, D. W. Setser and H. Horiguchi, J. Phys. Chem., Vol. 87, pp. 2199-2209, 1983.

22. R. Sauerbrey, W. Walter, F. K. Tittel and W. L. Wilson, Jr., J. Chem. Phys., Vol. 78, pp. 735-747, 1983.

23. Ch. A. Brau, "Rare Gas Halogen Excimers", in "Excimer Lasers", Second Edition, Topics in Applied Physics, Vol. 30, C. K. Rhodes, Ed., New York: Springer Verlag, 1984, Chap. 4.

24. S. R. Foltyn, Photonics Spectra, Vol. 20, p. 113, November, 1986.

25. N. R. Rajopadhye, V. A. Jogekar, V. N. Bhoraskar and S. V. Bhoresker, Solid State Comm., Vol. 60, p. 675, 1986.

PUBLICATIONS, PRESENTATIONS AND PATENTS

- F. A. Otter, Jr. and W. L. Nighan: Plasma Display Based on XeF Excimer Fluorescence. Presented at the 1985 International Display Research Conference, October 15-17, 1985, San Diego, CA.

- F. A. Otter, Jr. and W. L. Nighan: Plasma Display Based on XeF Excimer Fluorescence, IEEE Transactions on Electron Devices, Vol. ED-33, p. 1174 (1986).

- William L. Nighan and F. A. Otter, Jr.: An Optical Display from XeF Excimer Fluorescence. U.S. Patent Application filed October 1985. UTRC Docket No. R-3046.

PARTICIPATING SCIENTIFIC PERSONNEL

W. L. Nighan, Co-principal Investigator

F. A. Otter, Jr., Co-principal Investigator

Plasma Display Based on XeF Excimer Fluorescence

FRED A. OTTER, JR. AND WILLIAM L. NIGHAN, SENIOR MEMBER, IEEE

Abstract—Using a conventional ac plasma panel filled with a mixture containing Xe and F$_2$, visible emission from the XeF "excimer" molecule has been demonstrated at luminance levels higher than those observed for the standard Ne–Penning mixture/MgO surface combination operating at the same repetition frequency. A novel aspect of XeF excimer emission is the ability to change color by a simple change in mixture composition. Color can be varied continuously from pink through white to blue while retaining the luminance at an essentially constant level.

I. INTRODUCTION

A. Background

BECAUSE of the uniquely favorable electrical and optical properties of glow discharges in neon, practically all commercially available flat-panel plasma displays use a neon gas fill [1]. Indeed, in ac plasma panels the combination of the well known Ne–Penning mixture with the efficient durable MgO electron emitting layer results in a very low firing voltage (~ 100 V) and a relatively high luminous efficiency (~ 0.5 percent) [2], [3]. However, the neon transitions in the 580–700 nm region of the spectrum produce a reddish-orange color that is not suitable for all applications. Therefore, it would be highly desirable if gas mixtures capable of producing other colors could be found, while retaining the advantages of the now well developed ac plasma panel technology.

Since practically all gas discharges emit visible radiation, in principle, the easiest way to generate colors other than Ne orange is to change the gas mixture.[1] Ahearn and Sahni [4] investigated helium-based Penning mixtures containing a variety of heavy rare gas and/or atmospheric dopants. When excited using a conventional ac plasma panel (MgO surface), those mixtures exhibited electrical characteristics and luminance levels generally similar to Ne–Penning mixture, and violet, blue, and white colors were obtained. However, in order to produce luminance levels comparable to that of a Ne–Penning mixture excitation frequencies an order of magnitude higher were required. Thus, the luminous efficiency of such He-based mixtures is very low, a reflection of the fundamental fact that only a very small percentage of the fluorescence lies in the visible region.

[1] Other colors can be produced by using gas discharge generated electrons or UV radiation to excite phosphors. This aspect of flat-panel gas discharge displays will not be considered here (see [1] and references cited therein).

Sahni [5] also experimented with mercury-seeded argon mixtures. Blue and green Hg line emission was produced at luminance and efficiency levels significantly higher than those of Ne–Penning mixtures. Additionally, the firing voltage and memory margin were similar to those of conventional Ne-based mixtures. However, although the luminance and luminous efficiency levels were the highest ever observed for an ac plasma panel mixture, elevation of the panel temperature was required to optimize the Hg vapor concentration. Because of the strong dependence of Hg vapor pressure on temperature, both electrical and optical properties of the Ar/Hg panel exhibit variations in response to changes in temperature.

B. Excimer Mixtures

In recent years we have been exploring the feasibility of utilizing *excimer* molecule fluorescence for ac plasma panel applications [6], [7]. Excimers are excited species that are not stable in the ground electronic state and therefore are not present in the initial gas mixture. However, when a discharge is initiated excimers can be produced from certain mixture constituents, subsequently generating broadband visible emission upon spontaneous dissociative decay. Using an ac plasma panel of conventional design, in our prior work we demonstrated broadband blue-green emission from the Xe$_2$Cl excimer produced in mixtures containing Xe and Cl$_2$ [6], and broadband green emission from XeO produced in Xe–O$_2$ mixtures [7]. Although those early results were encouraging, the electrical and optical properties of Xe$_2$Cl and XeO mixtures do not rival those of the Ne–Penning mixture. However, the XeO emission is centered at 540 nm and is therefore exceptionally well matched to the response of the eye. For this reason XeO emission may be useful for limited plasma display applications for which green is especially desirable.

Recently, we have turned our attention to the XeF excimer which exhibits broadband emission centered at ~ 475 nm, and can be produced in mixtures containing Xe and F$_2$. Using a variety of mixtures we have demonstrated ac plasma panel luminance levels higher than those of the standard Ne–Penning mixture/MgO surface combination excited at the same repetition frequency (50 kHz). Although the experiments carried out to date require operating voltages higher than those of the Ne–Penning/MgO combination, resulting in luminous efficiency levels that are presently $\frac{1}{4}$ to $\frac{1}{10}$ times lower, the reduced efficiency level is predominantly the result of changes in the MgO electron emitting layer as modified by the pres-
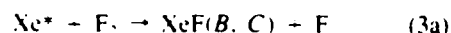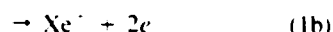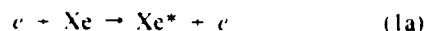
ence of F_2, rather than a fundamental limitation of the excimer gas mixture. Indeed, the luminous efficiency levels of Ne-Penning mixtures and XeF excimer mixtures are comparable for the same interior panel surface conditions. Moreover, XeF-based excimer fluorescence exhibits a range of colors continuously variable from pink through white to blue by way of very simple mixture changes. Thus, various colors, and possibly multicolor operation, may be possible within the basic framework of current ac plasma panel technology or reasonable extensions thereof. In the sections to follow the physics of XeF excimer formation is described briefly, along with our experimental results and a discussion of materials issues.
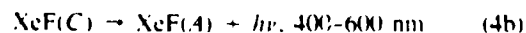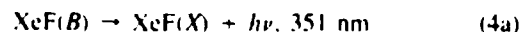
II. XeF Excimer Kinetics

A. XeF Formation

Throughout the past decade research interest in the physics of excimer molecules has been intense because of their utility as UV visible laser media. Of this class of molecules, the rare gas halides have received the most attention because of their unusually high formation efficiency when produced in an electric dicharge [8]. The primary rare gas halide transitions are in the UV region (~ 190-350 nm), with the exception of XeF which also exhibits a strong visible wavelength transition.

In a discharge excited mixture comprised of a rare gas background (RG) and small amounts (< 1 percent) of Xe and F_2, the two lowest energy ionic states of XeF, $B(\Omega = \frac{1}{2})$ and $C(\Omega = \frac{3}{2})$, are produced primarily by way of the following reaction sequence:

$$e + Xe \rightarrow Xe^* + e \qquad (1a)$$

$$\rightarrow Xe^+ + 2e \qquad (1b)$$

$$RG^* + Xe \rightarrow Xe^* + RG \qquad (2a)$$

$$\rightarrow Xe^+ + e + RG \qquad (2b)$$

$$Xe^* + F_2 \rightarrow XeF(B, C) + F \qquad (3a)$$

$$Xe^+ + F^- + RG \rightarrow XeF(B, C) + RG. \qquad (3b)$$

Ultraviolet and visible emission results from radiative transitions terminating on the dissociating XeF $X(\Omega = \frac{1}{2})$ and $A(\Omega = \frac{3}{2})$ states, respectively, i.e.,

$$XeF(B) \rightarrow XeF(X) + h\nu, 351 \text{ nm} \qquad (4a)$$

$$XeF(C) \rightarrow XeF(A) + h\nu, 400\text{-}600 \text{ nm} \qquad (4b)$$

The UV transition is of interest for laser applications [8] and will not be discussed further.[2]

B. XeF Vibrational Relaxation

Fig. 1 illustrates the XeF C and A potential curves of present interest. Reactions (3a) and (3b) result in the for-

[2]The 351 nm wavelength of the XeF($B \rightarrow X$) transition is significantly longer than the rare gas dimer emission (< 200 nm) often used to excite phosphors, and may be well suited for that application, either alone or in conjunction with the visible XeF($C \rightarrow A$) transition.
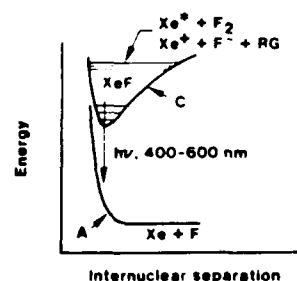

Fig. 1. Potential energy diagram illustrating XeF $C(\Omega = \frac{3}{2})$ and $A(\Omega = \frac{3}{2})$ states. Reactions 3a and 3b resulting in the formation of XeF(C) in high vibrational levels are indicated.

mation of XeF B and C in very high vibrational levels [9], [10] as indicated in the figure. Although not shown in Fig. 1, the XeF(B) potential curve is nearly coincident with that of the C state, with the C state lying approximately 0.1 eV lower in energy. For this reason, collisions with background rare gas atoms rapidly transfer energy between the vibrationally excited XeF B and C states, strongly favoring population buildup of XeF(C). Vibrational relaxation of XeF B and C, also the result of collisions with the background gas, occurs simultaneously with the XeF(C) population buildup due to B C mixing [9], [10]. For the high pressures typical of laser applications ($p > 2$ atm), nearly complete vibrational relaxation occurs in a time much less than the 100-ns radiative lifetime of XeF(C). In that case, a room-temperature Boltzmann vibrational distribution is established prior to XeF($C \rightarrow A$) radiative decay, and a broadband $C \rightarrow A$ emission spectrum centered at ~ 475 nm results, having a spectral width of ~ 70 nm (FWHM) [9]-[11]. However, for background gas pressures below 1 atm, the pressure range of interest for displays, the time required for XeF(C) vibrational relaxation is approximately the same as the 100-ns spontaneous decay time, with the result that the two processes occur simultaneously. Because higher vibrational levels are then involved in the $C \rightarrow A$ radiative process, and since the terminal XeF(A) state passes close to XeF(C) at reduced internuclear separation (Fig. 1), both shorter and longer wavelength emission results. The broadening effect on the visible spectrum when high XeF(C) vibrational levels contribute to the $C \rightarrow A$ fluorescence (i.e., $T_i \gg 300$ K) is illustrated in Fig. 2.

Vibrational relaxation of the XeF B and C state manifolds has been studied extensively [9], [10], and it has been found that for background gas pressures less than atmospheric Ne and He are relatively ineffective at relaxing the XeF(C) vibrational levels. However, Ar and Kr are very much more effective, particularly Kr. Since the presence of Ar or Kr is also compatible with efficient XeF formation [8], this indicates that the degree of XeF(C) vibrational relaxation (i.e., T_i), can be controlled by judicious selection of rare gas background constituents. Thus, XeF($C \rightarrow A$) spectral properties and therefore display color can be varied by simply changing the gas mixture.
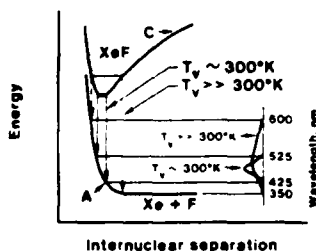
Fig. 2. Illustration of XeF(C → A) emission from low and high vibrational levels, and the broadening effect of the latter on the C → A spectral distribution.

Fig. 3. Illustration of the basic structure of the ac plasma display panel developed by Owens-Illinois (see Ref. 1). The MgF₂ passivation layer on the inner surface is indicated.

III. EXPERIMENTAL PROCEDURE

Two Owens-Illinois-developed ac plasma panels (sealed with a Penning gas mixture) were used in the present experiments. These test panels. illustrated in Fig. 3, have an electrode linewidth of 0.003 in (0.076 mm) on 0.019 in (0.48 mm) centers; the gas gap was 0.0038 in (0.096 mm). The electrical and optical properties of both sealed panels were fully characterized and found to be the same. One sealed panel was reserved as a reference standard for subsequent comparison with the other. which was opened and connected to a gas-handling system. The gas-handling system was constructed of bakeable ultrahigh-vacuum components pumped by a flexible pumping system that included a turbomolecular pump. a cryopump. and an ion pump. A magnetically rotated stirring vane ensured good mixing. and a residual gas analyzer permitted "before-and-after" analysis of gaseous contaminants. A simple square wave electrical driver of variable frequency was used for all experiments. The voltage rise time for the driver was less than 100 ns for the highest voltages. a time short compared with the period even at 200 kHz; the width of the current pulse was less than 300 ns.

A. Surface Passivation

Prior to experimentation with XeF mixtures. the interior surface of the test panel was fluorine passivated by filling the panel with several hundred torr of a He–5-percent F₂ mixture which remained in the panel for several days. We believe that this procedure converted the first few monolayers of the interior MgO surface to MgF₂, and passivated the gas-handling system as well. Regarding the effect of F₂ passivation on other interior materials such as the glass edge seal and the connection to the gas-handling system. subsequent experimentation revealed that the passivation was not perfect. However, temporal changes in electrical/optical properties, implying a change in F₂ concentration. were not observed until after several hours of continuous operation. which was more than satisfactory for the present purposes. Considering the nature of the experimental arrangement and the fact that panel interior materials were not intended to be F₂ compatible. we consider the observed behavior to be encouraging.

B. Emission Characterization

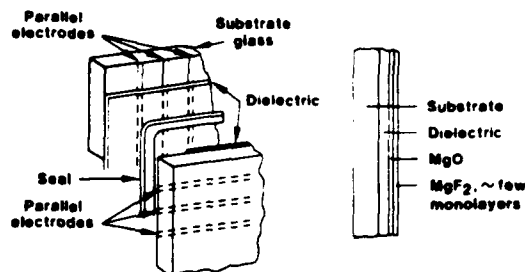1) Luminance: Measurements of luminance were made by collecting the light originating within a 0.006 in (0.152
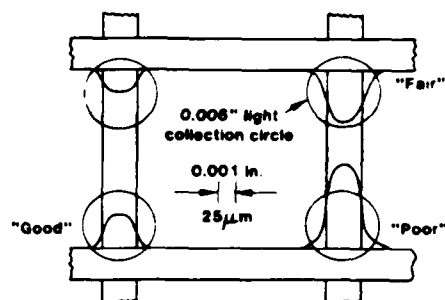

Fig. 4. Orientation of the light collection circle used in luminance measurements as described in the text. The shape and size of illuminated pixels relative to the measurement circle is also illustrated Various pixel shapes corresponding to our subjective evaluation of resolution quality are also indicated (see Table I and text).

mm) diameter circle centered near one pixel in the middle of a lighted 1.0 in (25.4 mm) × 0.5 in (12.7 mm) patch as illustrated in Fig. 4. This circle size was chosen because it represents the approximate limit of spatial resolution of the eye at a viewing distance of 21 in (53 cm) i.e., 1 minute of arc). A United Detector Technology (UDT) model 1120 Reflex Viewing Module was used with a 10× objective lens in order to image the light from the 0.006 in (0.152 mm) source circle onto a detector. Care was taken to orient the module so as to collect light emitted in a direction within a couple of degrees of normal to the panel surface. The detector, a UDT Model 255 Si detector (serial no. 864), was connected to a UDT model 550 Fiber Optic Power Meter. In front of the detector was a UDT Model 1157 photometric filter designed to give the system a wavelength sensitivity within ±2 percent of the CIE photopic eye response curve.

2) Spectral Properties: Emission spectral content was determined using a Jarrell-Ash 82-020 ½-m McPherson-type scanning monochrometer. The slits were set to correspond to an instrumental line width of 6 Å in order to produce sufficient detector signal in the broadband regions of the XeF(C → A) spectrum. Light was conducted from the panel to the monochrometer input slit using a 3-in-long light pipe. The transmittance of the light pipe was about 95 percent and was relatively constant over the wavelength range of interest. The detector was a UDT-555 "Photop" silicon photodiode with a built-in op-amp.

the output of which was recorded on a Moseley 680 chart recorder at the rate of 250 Å/min. The spectra were not corrected for the wavelength dependence of the detector sensitivity, which changed by only ~50 percent throughout the entire visible region.

IV. RESULTS

A. Emission Properties

After completion of the passivation procedure described previously, the passivated test panel was filled with a Ne–0.2-percent Xe-Penning mixture at a pressure of 500 torr. The orange color was found to be typical of the standard reference condition for this panel prior to passivation. However, the luminance was about 1.8 times higher and the pixel resolution was quite poor. In addition, the firing voltage increased by more than a factor of two reflecting the change in the electron emitting internal surface from MgO to MgF_2.

1) XeF Base Mixture: By increasing the Xe concentration to a few torr and after the addition of approximately 1-torr F_2 the color changed from orange to pink with an increase in luminance level. For example, for the mixture conditions of Fig. 5 the luminance level increased by more than a factor of two over that of the standard Ne-Penning mixture MgO surface combination operating at the same repetition rate (i.e., 50 kHz). Although the luminance was not unduly sensitive to the specific Xe and F_2 concentrations, the maximum luminance obtained to date occurred for Xe and F_2 pressures of about 5 and 1 torr, respectively. Thus, while the results shown in Fig. 5 are representative, they pertain to a less than optimum mixture.

Analysis of the spectrum of Fig. 6(a) shows that the addition of F_2 has very little effect on the Ne line emission compared to that of Ne-Penning/MgO combination, resulting in only a 20-percent decrease. However, in addition to the Ne emission, there appears the continuous XeF($C \rightarrow A$) excimer emission spanning most of the visible region. The XeF($C \rightarrow A$) spectral shape of Fig. 6(a) is typical of the emission from many XeF(C) vibrational levels (i.e., $T_v \gg$ 300 K). The combination of the Ne reddish-orange color with the nearly "white" XeF($C \rightarrow A$) emission results in the observed pink emission at a high luminance level.

2) Ar and Kr Addition: As explained previously, Ar and Kr are known to be much more effective than Ne at relaxing XeF(C) vibrational levels. Addition of 25-75 torr of Ar to the Ne-Xe-F_2 mixture of Fig. 6(a) was found to diminish the luminance somewhat and to change the color from pink to "white," often with either a slight pink or blue tint depending on the specific Ar concentration. Presented in Fig. 6(b) is a representative spectrum for a mixture containing Ar. Clearly the intensity of the Ne line emission is reduced significantly in this case and the shape of the $C \rightarrow A$ XeF emission is better defined, exhibiting a broad maximum centered at about 475 nm. With the addition of Kr in place of Ar, this trend is further accentuated. Fig. 6(c) shows that with 100-torr Kr added to a
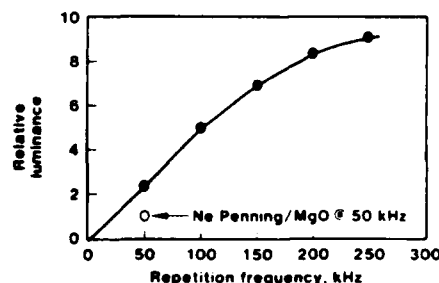

Fig. 5 Variation of the relative luminance with square wave repetition frequency for a representative (but not optimized) mixture comprised of Ne, 3-torr Xe, and 1-torr F_2 at a total pressure of 500 torr. For these conditions, pixel color was pink. The data points are normalized with respect to the luminance measured at 50 kHz for the standard Ne-Penning mixture/MgO surface combination of our reference panel
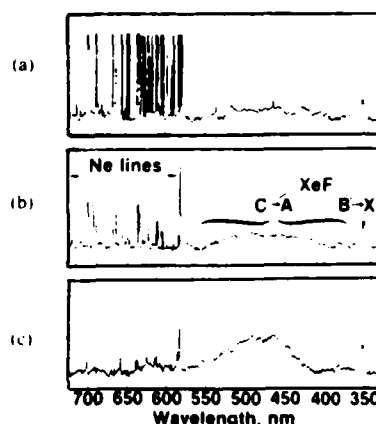

Fig. 6 Measured spectral properties for the following 500 torr mixtures (a) Ne, 3-torr Xe, and 1-torr F_2 (pink), (b) Ne, 3-torr Xe, 1-torr F_2, and 50-torr Ar ("white"), (c) Ne, 3-torr Xe, 1-torr F_2, and 100-torr Kr (blue)

Ne-Xe-F_2 mixture the Ne line emission is quenched almost completely and the XeF($C \rightarrow A$) emission exhibits the shape typical of nearly room-temperature Boltzmann distribution [9]-[11]. In this case, the emission appears blue and the measured luminance is essentially the same as that of the Ne-Penning mixture/MgO surface combination operating at the same repetition frequency.

The data of Fig. 6 show that the spectral shape, and therefore the color, of the XeF($C \rightarrow A$) emission can be changed by controlling the effective XeF(C) vibrational temperature, and by combining XeF($C \rightarrow A$) emission with Ne line emission. The chromaticity diagram of Fig. 7 illustrates the range of colors that have been observed and the approximate path through the color regions corresponding to the combined suppression of Ne line radiation and vibrational relaxation of XeF(C), both of which occur in response to addition of either Ar or Kr.

B. Electrical Properties

As mentioned previously, F_2 passivation of the initial MgO panel surface resulted in an increase in the firing voltage of a Ne-Penning mixture from ~100 to 250 V; the voltage margin was ~25 V for the initial MgO surface
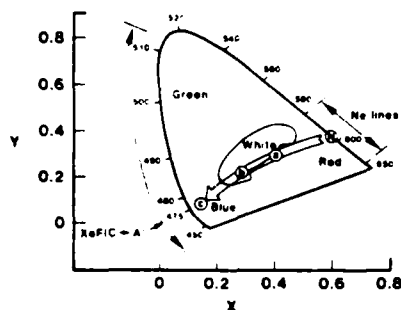
Fig 7. Adaptation of the 1931 CIE chromaticity diagram illustrating the range of colors observed from XeF-based display mixtures. The shape and location of the arrow are intended to show the approximate path through the various color regions in response to the addition of either Ar or Kr to our XeF "base" mixture. The letter "N" refers to a Ne-Penning mixture and a, b, and c refer to the observed colors corresponding to the spectra of Fig 6. The spectral width (FWHM) corresponding to a near-room-temperature XeF(C) vibrational distribution (blue emission) is also indicated
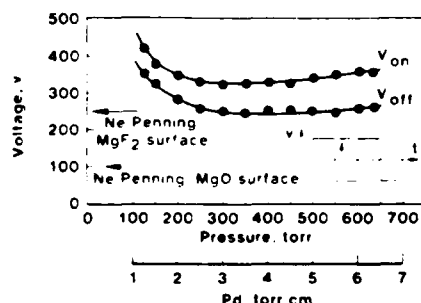

Fig 8 Firing (V_{on}) and extinction (V_{off}) voltages at a square wave repetition frequency of 50 kHz for a mixture comprised of Ne, 0.6-percent Xe, 0.2-percent F, and 5-percent Kr. For this mixture the emission was "white" at 500 torr.

Fig 9. Variation of firing (V_{on}) and extinction (V_{off}) voltages with repetition frequency corresponding to the mixture of Fig 8 at a pressure of 500 torr.

TABLE I
TYPICAL PROPERTIES OF XeF-BASED DISPLAY MIXTURES

Mixture	Relative luminance*	Mid-margin sustain voltage*	Voltage margin	Color	Resolution	Relative luminous efficiency*
Ne Penning MgO	1	100 V	25 V	Orange	Good	1
Ne Penning MgF₂	1.8	240	40	Orange	Poor	0.3
XeF base	2.1	260	90	Pink	Fair	0.3
Base + 25 T Kr	1.4	300	90	Pinkish white	Fair	0.15
Base + 50 T Kr	1.1	300	95	Bluish white	Good	0.12
Base + 100 T Kr	1.0	315	110	Blue	Good	0.1

*Relative luminance and relative luminous efficiency are measured relative to a standard test panel (Ne Penning mixture/MgO surface) operating at 50 kHz. The XeF Base mixture is comprised of Ne - 3 T Xe - 1 T F₂ at a total pressure of 500 Torr. the Ne partial pressure is reduced as Kr is added

V. SUMMARY AND DISCUSSION

A variety of colors ranging from pink through "white" to blue has been produced in an ac plasma panel by combining neon line emission with very broadband XeF excimer emission. A specific color or white can be obtained simply by changing the relative proportions of the rare gas mixture constituents. Moreover, although no attempt was made to optimize the concentrations of mixture constituents, the luminance levels of XeF-based mixtures were found to be at least equal to, and in some cases significantly higher than, those produced by the Ne-Penning mixture/MgO surface combination of our reference panel operated at the same repetition frequency.

The ability of our XeF mixtures to produce emission over a large portion of the visible spectrum suggests that additional flexibility can be obtained using various filters. Also, color ac plasma panel displays without the use of phosphors may be a possibility by combining the broadband visible emission of XeF-based mixtures with a fast optical switching device similar to the Tektronix liquid-crystal shutter, for example [12].

The dependence of ac panel ignition and extinction voltages on pd and the voltage memory margin are favorable for XeF mixtures. However, the voltage level is approximately three times higher than that of the standard Ne-Penning/MgO combination, due primarily to the nature of the fluoride inner surface. Thus, the luminous efficiency is lower than that of the standard panel. This fac-

and ~40 V for the passivated surface. For typical Ne-Xe-F₂ mixtures the firing voltage increased to ~300 V, but the extinction voltage did not change, with the result that the memory margin increased significantly to ~80-90 V. Addition of either Ar or Kr to the Ne-Xe-F₂ mixture further increased both the firing voltage and the margin, with little change in the extinction voltage.

Presented in Fig. 8 are the pixel firing and extinction voltages as a function of pressure for a representative mixture. The firing and extinction voltages and the margin exhibited a very weak dependence on pressure in the 200-700-torr range for all XeF mixtures examined. Additionally, Fig. 9 shows that the voltage margin exhibited no significant dependence on repetition frequency.

Electrical and optical properties of representative (but not optimized) XeF-based mixtures are summarized in Table 1, which also presents the comparative characteristics of our Ne-Penning/MgO reference panel, along with the properties of a Ne-Penning/MgF₂ panel. In the table, "poor" resolution refers to near overlap of lighted regions of adjacent pixels, "good" refers to a discharge small compared with pixel spacing, with "fair" referring to an intermediate condition, as illustrated in Fig. 4.
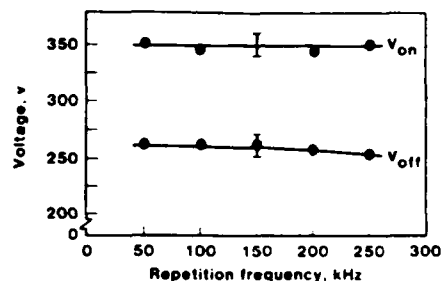
tor is partially offset for mixtures having a luminance that is higher than that of the standard system, thereby permitting operation at lower repetition frequency. Since increased luminance is likely as optimum XeF mixtures are identified, an improvement in luminous efficiency seems certain. Nonetheless, the higher operating voltage is disadvantageous and means to reduce the voltage levels are under consideration.

Without doubt, the key issue that will determine the viability of XeF-based displays is one of device lifetime using mixtures containing F_2. However, this problem is not as formidable as it might seem, an observation supported by our early experience with an F_2 passivated ac panel of conventional construction. During the last few years extensive research has been carried out by the laser community to identify optical and discharge materials that do not react with F_2, or can be thoroughly passivated against F_2 attack. In certain rare gas fluoride laser applications very long device lifetime is as important as is the case for displays, a problem that is greatly complicated by the fact that in lasers numerous materials are usually in contact with F_2. Additionally, laser system configuration is exceptionally complex compared with typical display envelopes. Indeed, ac plasma displays of the type used in this investigation feature very simple inner structures in which few different materials are actually in contact with the gas, and only one is in contact with the discharge. It seems reasonable that with minor changes in design or fabrication procedures, only a single material need be in contact with F_2. These issues are presently under investigation in parallel with a study of factors such as pixel-to-pixel interactions, pixel priming effects and other related characteristics that will ultimately determine the practicality of XeF-based mixtures as an information display medium.

ACKNOWLEDGMENT

REFERENCES

[1] L. F. Weber, "Plasma displays," in *Flat Panel Displays and CRTs*, L. E. Tannas, Jr., Ed. New York: Van Nostrand Reinhold, 1985, ch. 10.

[2] O. Sahni, C. Lanza, and W. E. Howard, "One-dimensional numerical simulation of ac discharges in a high-pressure mixture of Ne + 0.1% Ar confined to a narrow gap between insulated metal electrodes," *J. Appl. Phys.*, vol. 49, pp. 2365–2379, 1978.

[3] W. L. Nighan, "Basic kinetic processes in neon gas discharge displays," *IEEE Trans. Electron Devices*, vol. ED-28, pp. 625–630, 1981.

[4] W. E. Ahearn and O. Sahni, "The dependence of the spectral and electrical properties of AC plasma panels on the choice and purity of the gas mixture," in *SID Int. Symp. Dig. Tech. Papers*, pp. 44–45, 1978.

[5] O. Sahni, "Blue color AC plasma panel," in *SID Int. Symp. Dig. Tech. Papers*, pp. 82–83, 1980.

[6] W. L. Nighan and C. M. Ferrar, "Excimer fluorescence for plasma displays," *Appl. Phys. Lett.*, vol. 40, pp. 223–225, 1982.

[7] C. M. Ferrar and W. L. Nighan, "Excimer fluorescence for display applications," *IEEE Trans. Electron Devices*, vol. ED-30, pp. 439–443, 1983.

[8] Ch. A. Brau, "Rare gas halogen excimers," in *Excimer Lasers, Topics in Applied Physics*, 2nd ed., vol. 30, C. K. Rhodes, Ed. New York: Springer, 1984, ch. 4.

[9] H. C. Brashears, Jr. and D. W. Setser, "Transfer and quenching rate constants for XeF(B) and XeF(C) state in low vibrational levels," *J. Chem. Phys.*, vol. 76, pp. 4932–4946, 1982.

[10] Y. C. Yu, D. W. Setser, and H. Horiguchi, "Thermochemical and kinetic studies of the xenon halide B and C states in 0.5–5 atm of buffer gas," *J. Phys. Chem.*, vol. 87, pp. 2199–2209, 1983.

[11] R. Sauerbrey, W. Walter, F. K. Tittel, and W. L. Wilson, Jr., "Kinetic processes of electron beam generated XeF* and Xe₂F* excimers," *J. Chem. Phys.*, vol. 78, pp. 735–747, 1983.

[12] R. Vante, P. A. Johnson, Jr., and P. J. Bos, "ALC CRT field-sequential color display," in *SID Int. Symp. Dig. Tech. Papers*, pp. 28–29, 1983.

*

Fred A. Otter, Jr., was born in West Chester, PA, in 1928. He received the B.S. degree in engineering physics from Lehigh University in 1953, the A.M. degree in physics from Temple University in 1955, and the Ph.D. degree in physics from the University of Illinois in 1959.

He has been on the faculty at Ohio University (1959–1963) and Clarkson University (1969–1973). He has been at United Technologies Research Center from 1963 to 1969 and since 1973 where he is a Senior Principal Scientist. He is also a Visiting Professor of Physics at the University of Connecticut. His research activities have largely been experimental solid-state physics—superconductivity, surface science, and ion implantation.

Dr. Otter is a member of Sigma Xi, Phi Beta Kappa, Tau Beta Pi, the American Physical Society, and the Materials Research Society.

*

William L. Nighan (SM'85) was born in Philadelphia, PA, in 1938. He received the B.S. degree in engineering from the University of Dayton, Dayton, OH, in 1961 and the M.S. degree in engineering science from Northwestern University, Evanston, IL, in 1962.

Since 1962, he has been with United Technologies Research Center, East Hartford, CT, where he is a Senior Research Scientist. His primarily research activities have been in the areas of gas discharge physics, electric lasers, plasma displays and atomic and molecular physics.

Mr. Nighan is a member of Sigma Xi, Tau Beta Pi, and the American Physical Society.

END

JAN.
1988

DTIC